iodination of Tg, was added 24 h before the assay. After cells were exposed to $^{125}I$ (0.1 $\mu$Ci) for 1 h, radioiodide uptake was quantified. Approximately 3.41% of radioiodide taken up was retained in the protein fraction derived from BHP18–21v cells without depsipeptide (Fig. 5A). Tc-rNIS cells that expressed NIS, but not TPO or Tg, retained only about 2.11% of the iodide. This retention of radioiodide in untreated BHP18–21v and Tc-rNIS cells appeared to be nonspecific, because pretreatment of the cells with MMI did not significantly diminish the amount of protein-bound radioiodide. Treatment of BHP18–21v cells with 10 ng/ml depsipeptide significantly increased the amount of radioiodide bound to cellular proteins to almost 7.58%, compared with the cells pretreated with MMI ($P < 0.05$) (Fig. 5A). This organification induced by depsipeptide increased in a dose-dependent manner. Pretreatment of cells with MMI inhibited the increase in radioiodide organification.

In addition, to analyze whether re-expressed TPO could iodinate intracellular protein substrates, the molecular size of radioiodinated intracellular proteins was investigated. After BHP18–21v cells, which were pretreated with or without depsipeptide, were exposed to $^{125}I$ for 1 h, the intracellular proteins were separated by SDS-PAGE. In 3 ng/ml depsipeptide-treated cells, radiolabeled protein bigger than 210 kDa was detected, whereas it failed to produce radiolabeled protein without depsipeptide (Fig 5B).

These results indicate that TPO induced by HDACI was capable of facilitating iodide organification into protein substrates, in which the HDACI-induced expression of Tg played a crucial role on this effect.

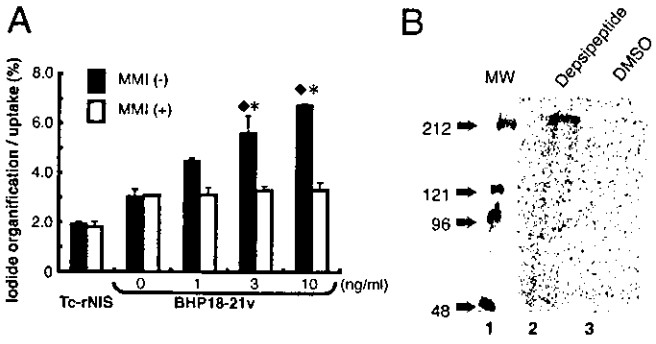


FIG. 5. Depsipeptide-induced iodide organification in BHP18–21v poorly differentiated thyroid cancer cells. A, Tc-rNIS cells were established from FRTL-Tc malignantly transformed thyroid cells transfected with NIS expression vector (8). Because the Tc-rNIS cell line overexpresses the NIS gene but does not express TPO and Tg, it was used as a negative control for iodide organification. BHP18–21v cells that were incubated in depsipeptide-containing medium with or without MMI were exposed to 0.2 $\mu$Ci/well $Na^{125}I$ for 1 h. The cells were washed in buffer, and radioactivity was counted. The radioactivity of $^{125}I$ bound to protein was determined by TCA precipitation. All data are expressed as the mean ± SEM (n = 6). ◆, $P < 0.05$, compared with nontreated with depsipeptide; *, $P < 0.05$, compared with MMI-treated cells. B, BHP18–21v cells were pretreated with or without 3 ng/ml depsipeptide for 48 h and exposed to 20 $\mu$Ci/dish $Na^{125}I$ for 1 h. Each sample (30 $\mu$g protein) was electrophoresed and analyzed using a BAS 2500 imaging analyzer (Fuji Film Co.). Lane 1, The molecular weight (MW) of the standard; lane 2, 3ng/ml depsipeptide-treated BHP18–21v cells; lane 3, DMSO-treated BHP18–21v cells.

*Depsipeptide leads to efficient iodide accumulation in vivo*

To evaluate the efficiency of depsipeptide *in vivo*, BHP18–21v cells were transplanted on the left flank of nude mice by sc injection of $1 \times 10^7$ cells. One week after transplantation, the cells formed small tumors at the injection site. The tumors grew very rapidly and were 1 cm in diameter 3 wk after transplantation. At this point, we injected 5 $\mu$g/g·d depsipeptide or DMSO in PBS ip for 4 d. To prevent radioiodide uptake by thyroid gland, mice were treated with L-$T_4$.

Autoradiographic imaging of the depsipeptide-treated mice displayed the accumulation of radioiodide in the physiological NIS-expressed organs, thyroid, stomach, and bladder. However, 48 h after, no accumulation was observed in stomach and bladder (Fig. 6A). In contrast, depsipeptide-treated tumors could accumulate $^{125}I$, as revealed by imaging at 12 and 48 h (Fig. 6A). Radioactivity in the tumors, thyroid, stomach, and liver were measured and were represented as a percent of the maximum uptake (Fig. 6A). The disappearance of radioiodide from the stomach paralleled the decrease in radioactivity from the liver. In contrast, the depsipeptide-treated tumors could reserve approximately 3.52% of maximum uptake 48 h after injection (Fig. 6A). The percentage of injected dose per gram of tissue of depsipeptide-treated tumors at 48 h after injection of $^{125}I$ was 0.70 ± 0.16%, whereas 0.14 ± 0.04% of radioiodide remained in DMSO-treated tumors ($P < 0.05$). In addition, radioiodide measurement by whole-body scanning showed that values of 5.95 ± 0.39% and 1.49 ± 0.93% of whole-body retention at 48 h were detected in tumors treated with depsipeptide and DMSO, respectively. Radioiodide accumulation in thyroid glands gradually increased and peaked 48 h after injection.

To examine the time-dependent accumulation of $^{125}I$ in these mice, the tumor/liver $^{125}I$ concentration ratio was measured at 3, 12, and 48 h after injection of 10 $\mu$Ci $Na^{125}I$. Three hours after the injection, there was no significant difference between the tumor/liver ratios in depsipeptide- and DMSO-treated mice. At 12 and 48 h, the tumor/liver $^{125}I$ concentration ratio was 4.56 ± 1.35 and 11.03 ± 3.37 in depsipeptide-treated mice, respectively, whereas that in DMSO-treated mice was 0.48 ± 3.37 and 1.57 ± 0.33, respectively. There was a significant difference in the tumor/liver $^{125}I$ concentration ratio between the depsipeptide-treated and DMSO-treated mice after 12 h ($P < 0.05$) (Fig. 6B).

To analyze iodide organification *in vivo*, we measured protein-bound radioiodide in xenotransplanted tumors. A total of 10 $\mu$Ci of $Na^{125}I$ was injected into the mice treated with depsipeptide or DMSO. The removed tumors were disrupted, and intracellular protein was extracted. The protein-bound radioiodide in depsipeptide-treated mice was 36.74 ± 7.0 cpm/mg, whereas that in DMSO-treated mice was 6.16 ± 3.6 cpm/mg ($P < 0.05$) (Fig. 6C).

To investigate the effects of the HDACI on the expression of NIS, TPO, Tg, and TSH-R *in vivo*, we analyzed the mRNA levels of these thyroid-specific genes in depsipeptide- or DMSO-treated tumors using quantitative real-time PCR (Table 2). The mice were treated with 5 $\mu$g/g·d depsipeptide or DMSO in PBS for 4 d. In DMSO-treated mice, NIS, TPO, Tg, and TSH-R mRNA were not observed. Re-expression of NIS, TPO, and Tg was detected in depsipeptide-treated tumors,

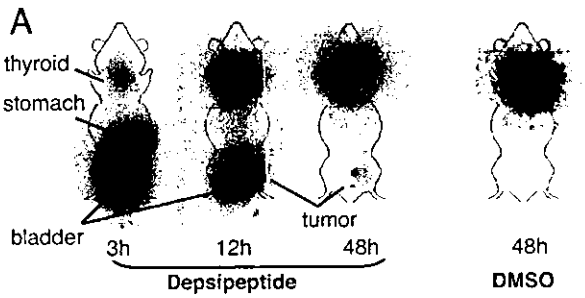


| | Iodide uptake (% of maximum uptake) | | |
|---|---|---|---|
| | 3 h | 12 h | 48 h |
| thyroid | 29.42 | 46.93 | 100.00 |
| tumor | 100.00 | 34.50 | 3.52 |
| stomach | 100.00 | 2.31 | 0.04 |
| liver | 100.00 | 9.42 | 0.25 |

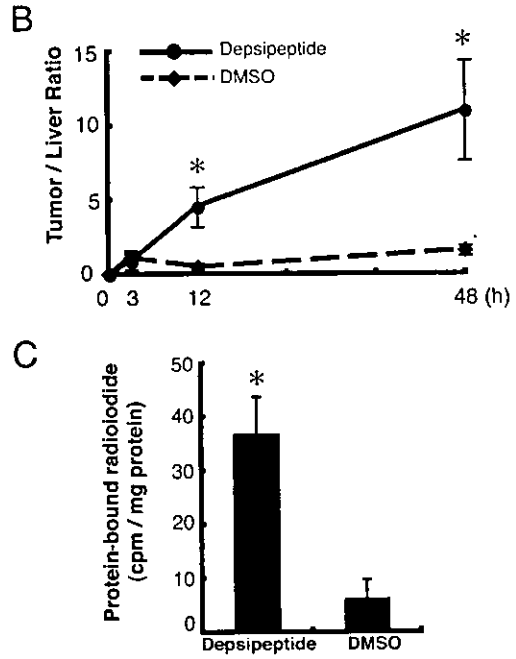


FIG. 6. Induction of intratumoral radioiodide accumulation by depsipeptide *in vivo*. BHP18–21v cells were transplanted on the left flank of nude mice by sc injection. Mice were treated with L-$T_4$ to avoid massive uptake by the thyroid. A total of 5 μg/g·d depsipeptide was injected ip for 4 d. After the injection of 10 μCi of $^{125}I$, the radioactivity from the mice was analyzed using a BAS2500 imaging analyzer. A, Typical images 3, 12, and 48 h after the injection. Thyroid, stomach, and bladder are observed by their physiologic uptake. Radioactivity from the tumors, thyroid, stomach, and liver was measured and represented as a percent of the maximum uptake. B, After calculating the amounts of radioiodide uptake per tissue weight, tumor/liver radioiodide uptake ratio was elevated. C, The intratumoral radioactivity of $^{125}I$ bound to protein was determined by TCA precipitation. Radioactivity was measured with a γ-counter and normalized by dividing the amounts of proteins weight. All data are expressed as the mean ± SEM (n = 6). *, $P < 0.05$, compared with DMSO-treated tumors.

whereas the induction of TSH-R mRNA was not observed. These results clearly demonstrated that depsipeptide could induce the expression of thyroid-specific genes that is necessary for effective cell processing of iodide, and this depsipeptide-induced radioiodide uptake is TSH-independent.

*HDACI stimulates TTF-1 gene expression*

Expression of thyroid-specific genes (NIS, TPO, and Tg) is modulated, in part, by the interaction of the TTF-1 and Pax-8, thyroid-specific transcription factors with their respective promoters (16). To analyze the mechanisms by which the HDACI-induced re-expression of thyroid-specific genes took place, we examined changes in the expression of the thyroid-specific transcription factor after treatment of HDACI using RT-PCR. In untreated ARO cells, only faint expression of TTF-1 mRNA was detected (Fig. 7). Depsipeptide treatment in this cell line caused a dose-dependent increase in expression of the TTF-1 gene. Maximum gene expression was obtained at 10 ng/ml depsipeptide. However, depsipeptide were unable to restore the expression of Pax-8 mRNA that was lost in ARO cells (data not shown). In BHP18–21v cells, which express Pax-8 but not TTF-1 mRNA, depsipeptide induced the expression of TTF-1 mRNA in a dose-dependent manner. Maximum TTF-1 gene expression was observed in cells incubated with 10 ng/ml depsipeptide for 24 h (Fig. 7A).

We also analyzed time-dependency of HDACI-induced expression of the TTF-1 gene. After incubation with 3 ng/ml depsipeptide, TTF-1 mRNA levels reached a maximum after 24 h and after 12 h in BHP18–21v and ARO cells, respectively. Conversely, Pax-8 mRNA levels significantly decreased in BHP18–21v cells after incubation with depsipeptide.

*Cycloheximide diminishes depsipeptide-induced NIS gene expression and enhances the TPO and Tg gene expression*

HDACI directly activates the regulatory machinery of transcription via an increase of acetylated histones (38), but also can modulate expression of certain transcription factors, including TTF-1 (Fig. 7). To investigate whether new protein synthesis was necessary for induction of thyroid-specific genes in depsipeptide-treated BHP18–21v and ARO cells, we measured expression of thyroid-specific genes with or without cycloheximide (Biomol Corp., Plymouth Meeting, PA) treatment. After BHP18–21v and ARO cells were incubated with 3 ng/ml depsipeptide in the presence or absence of 30 μg/ml cycloheximide for 24 h, expression levels of thyroid-specific genes were quantified by real-time RT-PCR. Cycloheximide partly, but significantly, inhibited the depsipeptide-induced up-regulation of NIS mRNA (Fig. 8); approximately 70% of induced NIS gene expression was abolished. Thus, a portion of depsipeptide-induced up-regulation of NIS mRNA required ongoing protein synthesis.

The faint increases in TPO and Tg mRNA levels were observed in the presence of cycloheximide without depsipeptide (Fig. 8). The presence of cycloheximide led to elevated expression levels of TPO mRNA induced by 3 ng/ml depsipeptide in BHP18–21v and ARO cells. In depsipeptide-treated BHP18–21v and ARO cells, cycloheximide similarly induced 30.0-fold and 16.8-fold increases in Tg mRNA levels, respectively. These results suggested that depsipeptide-

**TABLE 2.** The expression of NIS, TPO, Tg, and TSH-R mRNA in xenotransplanted BHP18-21v cells isolated from DMSO-treated mice and depsipeptide-treated mice

| | NIS | TPO | Tg | TSH-R |
|---|---|---|---|---|
| Depsipeptide | $2.84 \times 10^{-3} \pm 0.001^a$ | $1.11 \times 10^{-1} \pm 0.047^a$ | $7.67 \times 10^{-1} \pm 0.195^a$ | 0 |
| DMSO | 0 | 0 | 0 | 0 |

Each group of mice was treated with DMSO or depsipeptide for 4 d. Amounts of NIS, TPO, Tg, and TSH-R mRNA were determined by quantitative real-time RT-PCR with 100 ng cDNA in duplicate. All data are ratio to GAPDH mRNA level and expressed as the mean ± SEM.
$^a P < 0.05$.

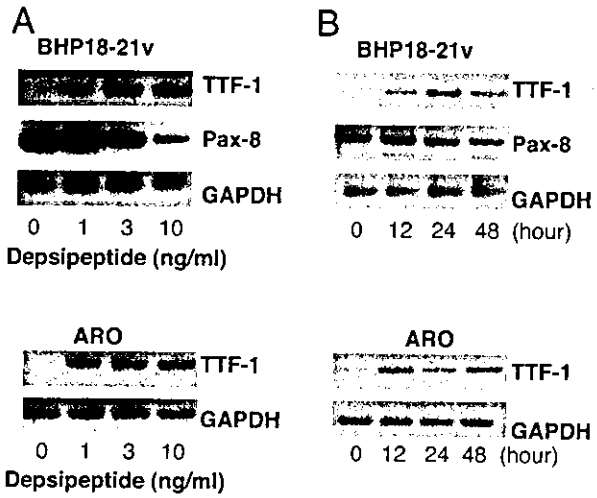


FIG. 7. Effect of depsipeptide on the expression of thyroid-specific transcription factors. Amounts of TTF-1, Pax-8, and GAPDH mRNA were determined by RT-PCR. A, BHP18–21v and ARO cells were incubated with 1, 3, or 10 ng/ml of depsipeptide for 24 h. B, Time-course analysis was performed by RT-PCR. TTF-1 and Pax-8 gene expression was analyzed using BHP18–21v and ARO cells incubated with 3 ng/ml depsipeptide for 12, 24, or 48 h.

induced re-expression of TPO and Tg genes was not mediated by newly produced-transcription factors.

*Depsipeptide exhibits cytotoxic effect against BHP18–21v and ARO cells in vitro*

We examined the effect of depsipeptide on viabilities of ARO and BHP18–21v cells. In both cell lines, 1 ng/ml depsipeptide exhibited no cytotoxicity. Administration of 3 ng/ml depsipeptide was not cytotoxic in BHP18–21v, whereas 51% of ARO cells resulted in cell death ($P < 0.05$). Almost 90% cell death was observed in ARO and BHP18–21v cells treated with 10 ng/ml depsipeptide ($P < 0.05$) (Fig. 9). In comparison with depsipeptide-induced expression of thyroid-specific genes, higher concentrations of depsipeptide were required for the cytotoxic effect.

## Discussion

Radioiodide therapy of thyroid carcinoma with preserved ability of trapping and concentration of iodide is not effective in poorly differentiated or anaplastic thyroid cancers, in which thyroid-specific gene expression is lacking (6, 39). In the present study, we showed that exposure of poorly differentiated papillary thyroid BHP18–21v cells and anaplastic thyroid ARO cells to the HDACI induced the expression of NIS, TPO, and Tg mRNAs. We also demonstrated immunoreactive NIS, TPO, and Tg proteins in HDACI-treated

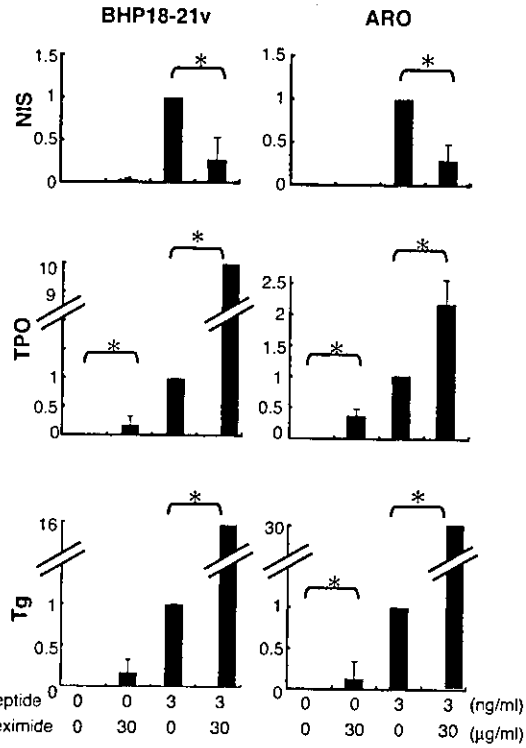


FIG. 8. Effect of cycloheximide on regulation of thyroid-specific genes in depsipeptide-treated BHP18–21v and ARO cells. BHP18–21v and ARO cells were incubated with 1, 3, or 10 ng/ml depsipeptide in the presence or absence of cycloheximide for 24 h. Total RNA was isolated in four independent samples. Amounts of NIS, TPO, and Tg mRNA were determined by quantitative real-time RT-PCR with 100 ng cDNA in triplicate. Relative quantification of target cDNA was determined by arbitrarily setting the control value from 3 ng/ml depsipeptide-incubation samples to 1. All data are expressed as the mean ± SEM. *, $P < 0.05$.

BHP18–21v and ARO cells. We provided further evidence clearly demonstrating that HDACI-treated cancer cells increased their radioiodide uptake and prolonged radioiodide retention in depsipeptide-treated tumors *in vitro* and *in vivo*.

We have reported that, despite radioiodide accumulation, $Na^{131}I$ did not significantly change the volume of experimental tumors formed by rat undifferentiated thyroid cells with or without transfection with NIS (8). In that study, extracorporeal measurement of radioactivity in the tumors revealed that $^{125}I$ accumulation peaked at 90 min and decreased to 50% 6 h after injection *in vivo*. In contrast, $^{125}I$ uptake in thyroid glands gradually increased and peaked 48 h after injection. These results demonstrated the differences between NIS-expressed tumor and thyroid glands in time-dependent iodide accumulations may be related to their

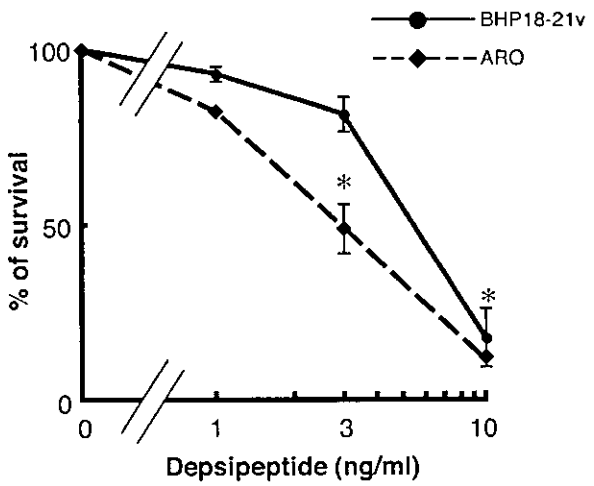


FIG. 9. Effect of depsipeptide on cell viability in BHP18–21v and ARO cells. BHP18–21v and ARO cells were incubated with 1, 3, or 10 ng/ml for 48 h. Cell viability were analyzed using a Cell Counting Kit. Survival of cells is presented as a percentage of the absorbance with depsipeptide-treated cells divided by that with cells not exposed to depsipeptide. All data are expressed as the mean ± SEM. *, $P < 0.05$, compared with untreated cells.

abilities to organify iodide. These results indicate that cytotoxic efficacy of radioiodide may be limited by the radioiodide efflux, and that enhancing the intracellular retention of iodide is necessary for effective radioiodide therapy. Rapid washout of radioiodide from tumors and low binding of radioiodide are probably consequences of the absence of TPO and Tg gene expression.

Our present study is the first report showing simultaneous induction of NIS, TPO, and Tg gene expression and iodide organification by HDACI in undifferentiated papillary thyroid cancer cells *in vitro*. Furthermore, we demonstrated HDACI-induced radioiodide accumulation in tumors formed with thyroid cancer cells *in vivo*. Certain reagents or transcription factors have been found to induce re-expression of thyroid-specific genes. Fagin *et al.* (40) reported that papillary thyroid cancer cells transfected with wild-type p53 showed re-expression of TPO mRNA and protein. Re-expression of Pax-8 mRNA, which specifically activates the TPO promoter, also was demonstrated. Schmutzler (41) reported that all-trans retinoic acid increased NIS mRNA in human follicular thyroid cancer cells. Venkataraman *et al.* (42) similarly found that 5-azacytidine could restore the expression of NIS mRNA and radioiodide uptake in benign thyroid adenoma cells. Kitazono *et al.* (43, 44) reported that HDACI induced the re-expression of NIS and Tg mRNA in human anaplastic thyroid cancer cells.

TPO is the primary enzyme involved in iodide organification (45), being active at the apical pole of the thyrocytes, where oxidizing $H_2O_2$ is produced (46). It has been shown that TPO can also be active intracellularly in the presence of $H_2O_2$, leading to low levels of intracellularly iodinated proteins (47). Recently, Huang *et al.* (48) reported that an increase of iodide organification was observed in NIS- and TPO-cotransfected lung cancer cells. Boland *et al.* (49) reported that the levels of iodide organification obtained were too low to increase the iodide retention time in the thyroid cancer cells cotransfected with NIS and TPO. These reports suggested that expression of Tg was required for the effective iodide retention and organification. In this report, radiolabeled protein greater than 210 kDa was specifically observed, and iodide organification was detected in depsipeptide-treated thyroid cancer cells. These results supported the hypothesis that the induction of iodide organification may require combined expression of NIS, TPO, and Tg, and TPO induced by depsipeptide was capable of facilitating iodide organification into protein substrates, in which the HDACI-induced expression of Tg could play a crucial role on this effect. However, the fact that smear bands appeared suggests a possibility that some other protein substrates might be iodinated in the process of depsipeptide-induced iodide organification.

In the present report, we demonstrated that inhibition of histone deacetylation by HDACI induced the expression of thyroid-specific genes in thyroid cancer cells. Acetylation and deacetylation of histones plays a significant role in regulation of gene transcription in many cell types (38). Histone acetylation alters nucleosomal conformation, which in turn can increase accessibility of transcriptional regulatory proteins to chromatin templates (50). HDAC oppose these events by catalyzing removal of acetyl groups from the amino-terminal lysine residues of core nucleosomal histones (51). Although HDACI act on the general regulatory machinery of transcription, our results demonstrated that HDACI do not do so nonspecifically. For example, HDACI did not increase expression of the GAPDH and Pax-8 genes (Figs. 1 and 7).

TTF-1 and Pax-8 are major transcription factors regulating the Tg and TPO promoter activity positively. We observed that depsipeptide could increase in the expression level of TTF-1. In contrast, the expression levels of Pax-8 mRNA were decreased in depsipeptide-treated BHP18–21v cells, and were not observed in depsipeptide-treated ARO cells. We detected that overexpression of TTF-1 using an adenovirus vector inhibited the expression of Pax-8 mRNA in BHP18–21v cells (12, 13, 16–19). Therefore, we suspect that re-expressed TTF-1 induced by HDACI could influence the reduction of Pax-8 mRNA in BHP18–21v cells. Because depsipeptide exhibited an opposite effect on the expression of TTF-1 and Pax-8, we studied the effect of cycloheximide on Tg and TPO gene expression to determine whether HDACI acts through newly synthesized transcription factors or, instead, directly activates the transcriptional machinery for thyroid-specific genes. Figure 8 shows that the presence of cycloheximide did not decrease the levels of HDACI-induced TPO or Tg expression. These results suggested that HDACI-induced re-expression of TPO or Tg genes was not mediated by newly produced *trans*-activating factors.

Moreover, cycloheximide increased the expression of TPO and Tg mRNA in depsipeptide-treated and untreated cells. We suspect that unknown proteins inhibit TPO and Tg gene expression in cancer cells, and cycloheximide might block the synthesis of these unknown proteins.

In contrast, this study revealed that up-regulation of the NIS gene partly involved newly produced proteins, presumably some transcription factors. In our study, HDACI solely induced expression of TTF-1. Kitazono *et al.* (52) demonstrated that TTF-1 gene was re-expressed in thyroid cancer

cells by simultaneous treatment with depsipeptide and 8-Br-cAMP. In the rat NIS gene, TTF-1 was shown to activate the rat NIS promoter by a direct interaction with its proximal enhancer region (18). Further, Taki *et al.* (22) found a TTF-1-binding site in the human NIS upstream enhancer, but TTF-1 did not act as a *trans*-activating factor on the human NIS upstream element. Schmitt *et al.* (53) also reported that transcription of a TTF-1 expression vector showed no effect on luciferase activity driven by the 9-kb NIS promoter. We presently suspect that an unidentified protein activated by HDACI was involved in NIS gene induction. It is also possible that newly synthesized TTF-1 is involved in the induction of NIS gene expression via interactions of the NIS gene other than these previously investigated.

HDACI was identified as an antitumor agent (54). In human bladder cancer cells, HDACI induced apoptosis, which might be related to the re-expression of p21, c-myc, and gelsolin genes (11). In human breast cancer cells, increased p21, phosphorylation of Bcl-2, and apoptosis have been observed after treatment with depsipeptide (55). In the case of thyroid cancer, Greenberg *et al.* (56) demonstrated that 500 nM TSA induced apoptosis and cell-cycle arrest in anaplastic thyroid cancer cells. In our study, poorly differentiated and anaplastic thyroid cancer cells treated with 30 ng/ml (99 nM) TSA showed re-expression of the thyroid-specific genes that are required for effective radioiodide therapy (Fig. 1B). HDACI previously have been shown to simultaneously induce differentiation and apoptosis, as well as cell-cycle arrest, in breast cancer, bladder cancer, and leukemia in mice (11, 54, 55, 57, 58). In this study, 10 ng/ml depsipeptide could induce cell-death concomitantly with iodide accumulation in poorly differentiated and anaplastic thyroid cancer cells (Figs. 3 and 9). It is reasonable to speculate that the depsipeptide-induced cell-death can be a beneficial effect, from the standpoint of cancer therapy using radioiodide.

Depsipeptide, a strong inhibitor of histone deacetylase, is currently in phase I trials in the United States. These trials suggest that the maximum tolerated plasma concentration is about 472.6 ng/ml (59). In this study we confirmed that a low-dose depsipeptide concentration (1–10 ng/ml) induced iodide uptake and organification in poorly differentiated thyroid cancer cells. Furthermore, depsipeptide-treated tumors could specifically accumulate radioiodide, as revealed by imaging experiments and radioiodide concentration *in vivo*. Schlumberger *et al.* (60) reported that the presence of $^{131}I$ uptake that could be detected using whole-body scanning was one of the most important prognostic factors in thyroid cancer patients with metastases. Although the tumoral uptake was dependent on tumor size, it was reported that most of positive scans were above 0.7% of whole-body retention 48 h after administration of radioiodide (61, 62). In the present study, whole-body scanning performed 48 h after injection (Fig. 6A) showed that depsipeptide- and DMSO-treated tumors could accumulate 5.95 ± 0.39% and 1.49 ± 0.93% of whole-body retention, respectively ($P < 0.01$). We therefore speculate that this HDACI-induced iodide retention may confer some therapeutic effects on poorly differentiated and anaplastic thyroid carcinoma.

## Acknowledgments

We are grateful to Fujisawa Pharmaceutical Co. Ltd. for providing depsipeptide (FR901228).

Received September 19, 2003. Accepted February 9, 2004.

Address all correspondence and requests for reprints to: Tetsuro Kobayashi, M.D., Ph.D., Professor and Chairman, Third Department of Internal Medicine, Faculty of Medicine, University of Yamanashi, 1110 Tamaho, Yamanashi 409-3898, Japan. E-mail: tetsurou@yamanashi.ac.jp.

## References

1. **Fraker D, Skarulis MC, Livolsi V** 1997 Thyroid tumors. In: De Vita VT, Hellmam S, Rosenberg SA, eds. Cancer principles and practice of oncology. 5th ed. Philadelphia: Lippincott-Raven; 1629–1652
2. **Nel CJ, van Heerden JA, Goellner JR, Gharib H, McConahey WM, Taylor WF, Grant CS** 1985 Anaplastic carcinoma of the thyroid: a clinicopathologic study of 82 cases. Mayo Clin Proc 60:51–58
3. **Venkatesh YS, Ordonez NG, Schultz PN, Hickey RC, Goepfert H, Samaan NA** 1990 Anaplastic carcinoma of the thyroid. A clinicopathologic study of 121 cases. Cancer 66:321–330
4. **DeGroot LJ, Kaplan EL, McCormick M, Straus FH** 1990 Natural history, treatment, and course of papillary thyroid carcinoma. J Clin Endocrinol Metab 71:414–424
5. **Beierwaltes WH** 1978 The treatment of thyroid carcinoma with radioactive iodine. Semin Nucl Med 8:79–94
6. **Schlumberger M, Tubiana M, De Vathaire F, Hill C, Gardet P, Travagli JP, Fragu P, Lumbroso J, Caillou B, Parmentier C** 1986 Long-term results of treatment of 283 patients with lung and bone metastases from differentiated thyroid carcinoma. J Clin Endocrinol Metab 63:960–967
7. **Schlumberger MJ** 1998 Papillary and follicular thyroid carcinoma. N Engl J Med 338:297–306
8. **Shimura H, Haraguchi K, Miyazaki A, Endo T, Onaya T** 1997 Iodide uptake and experimental 131I therapy in transplanted undifferentiated thyroid cancer cells expressing the Na+/I− symporter gene. Endocrinology 138:4493–4496
9. **Nagy L, Kao HY, Chakravarti D, Lin RJ, Hassig CA, Ayer DE, Schreiber SL, Evans RM** 1997 Nuclear receptor repression mediated by a complex containing SMRT, mSin3A, and histone deacetylase. Cell 89:373–380
10. **Hong L, Schroth GP, Matthews HR, Yau P, Bradbury EM** 1993 Studies of the DNA binding properties of histone H4 amino terminus. Thermal denaturation studies reveal that acetylation markedly reduces the binding constant of the H4 "tail" to DNA. J Biol Chem 268:305–314
11. **Richon VM, Sandhoff TW, Rifkind RA, Marks PA** 2000 Histone deacetylase inhibitor selectively induces p21WAF1 expression and gene-associated histone acetylation. Proc Natl Acad Sci USA 97:10014–10019
12. **Guazzi S, Price M, De Felice M, Damante G, Mattei MG, Di Lauro R** 1990 Thyroid nuclear factor 1 (TTF-1) contains a homeodomain and displays a novel DNA binding specificity. EMBO J 9:3631–3639
13. **Mizuno K, Gonzalez FJ, Kimura S** 1991 Thyroid-specific enhancer-binding protein (T/EBP): cDNA cloning, functional characterization, and structural identity with thyroid transcription factor TTF-1. Mol Cell Biol 11:4927–4933
14. **Ikuyama S, Niller HH, Shimura H, Akamizu T, Kohn LD** 1992 Characterization of the 5′-flanking region of the rat thyrotropin receptor gene. Mol Endocrinol 6:793–804
15. **Zannini M, Francis-Lang H, Plachov D, Di Lauro R** 1992 Pax-8, a paired domain-containing protein, binds to a sequence overlapping the recognition site of a homeodomain and activates transcription from two thyroid-specific promoters. Mol Cell Biol 12:4230–4241
16. **Damante G, Di Lauro R** 1994 Thyroid-specific gene expression. Biochim Biophys Acta 1218:255–266
17. **Shimura H, Okajima F, Ikuyama S, Shimura Y, Kimura S, Saji M, Kohn LD** 1994 Thyroid-specific expression and cyclic adenosine 3′,5′-monophosphate autoregulation of the thyrotropin receptor gene involves thyroid transcription factor-1. Mol Endocrinol 8:1049–1069
18. **Endo T, Kaneshige M, Nakazato M, Ohmori M, Harii N, Onaya T** 1997 Thyroid transcription factor-1 activates the promoter activity of rat thyroid Na+/I− symporter gene. Mol Endocrinol 11:1747–1755
19. **Kimura S** 1997 Role of the thyroid-specific enhancer-binding protein in transcription, development and differentiation. Eur J Endocrinol 136:128–136
20. **Macchia PE, Mattei MG, Lapi P, Fenzi G, Di Lauro R** 1999 Cloning, chromosomal localization and identification of polymorphisms in the human thyroid transcription factor 2 gene (TITF2). Biochimie 81:433–440
21. **Ohno M, Zannini M, Levy O, Carrasco N, di Lauro R** 1999 The paired-domain transcription factor Pax8 binds to the upstream enhancer of the rat sodium/iodide symporter gene and participates in both thyroid-specific and cyclic-AMP-dependent transcription. Mol Cell Biol 19:2051–2060
22. **Taki K, Kogai T, Kanamoto Y, Hershman JM, Brent GA** 2002 A thyroid-specific far-upstream enhancer in the human sodium/iodide symporter gene requires Pax-8 binding and cyclic adenosine 3′,5′-monophosphate response

element-like sequence binding proteins for full activity and is differentially regulated in normal and thyroid cancer cells. Mol Endocrinol 16:2266–2282
23. **Plachov D, Chowdhury K, Walther C, Simon D, Guenet JL, Gruss P** 1990 Pax8, a murine paired box gene expressed in the developing excretory system and thyroid gland. Development 110:643–651
24. **Shimura H, Suzuki H, Miyazaki A, Furuya F, Ohta K, Haraguchi K, Endo T, Onaya T** 2001 Transcriptional activation of the thyroglobulin promoter directing suicide gene expression by thyroid transcription factor-1 in thyroid cancer cells. Cancer Res 61:3640–3646
25. **Esposito C, Miccadei S, Saiardi A, Civitareale D**1998 PAX 8 activates the enhancer of the human thyroperoxidase gene. Biochem J 331:37–40
26. **Ohta K, Pang XP, Berg L, Hershman JM** 1997 Growth inhibition of new human thyroid carcinoma cell lines by activation of adenylate cyclase through the β-adrenergic receptor. J Clin Endocrinol Metab 82:2633–2638
27. **Van Herle AJ, Agatep ML, Padua 3rd DN, Totanes TL, Canlapan DV, Van Herle HM, Juillard GJ** 1990 Effect of 13 *cis*-retinoic acid on growth and differentiation of human follicular carcinoma cells (UCLA R0 82 W-1) *in vitro*. J Clin Endocrinol Metab 71:755–763
28. **Endo T, Shimura H, Saito T, Onaya T** 1990 Cloning of malignantly transformed rat thyroid (FRTL) cells with thyrotropin receptors and their growth inhibition by 3′,5′-cyclic adenosine monophosphate. Endocrinology 126:1492–1497
29. **Endo T, Kaneshige M, Nakazato M, Kogai T, Saito T, Onaya T** 1996 Autoantibody against thyroid iodide transporter in the sera from patients with Hashimoto's thyroiditis possesses iodide transport inhibitory activity. Biochem Biophys Res Commun 228:199–202
30. **Bidart JM, Lacroix L, Evain-Brion D, Caillou B, Lazar V, Frydman R, Bellet D, Filetti S, Schlumberger M** 2000 Expression of Na+/I− symporter and Pendred syndrome genes in trophoblast cells. J Clin Endocrinol Metab 85:4367–4372
31. **Wingo ST, Ringel MD, Anderson JS, Patel AD, Lukes YD, Djuh YY, Solomon B, Nicholson D, Balducci-Silano PL, Levine MA, Francis GL, Tuttle RM** 1999 Quantitative reverse transcription-PCR measurement of thyroglobulin mRNA in peripheral blood of healthy subjects. Clin Chem 45:785–789
32. **Agretti P, Chiovato L, De Marco G, Marcocci C, Mazzi B, Sellari-Franceschini S, Vitti P, Pinchera A, Tonacchera M** 2002 Real-time PCR provides evidence for thyrotropin receptor mRNA expression in orbital as well as in extraorbital tissues. Eur J Endocrinol 147:733–739
33. **Saito T, Endo T, Kawaguchi A, Ikeda M, Katoh R, Kawaoi A, Muramatsu A, Onaya T** 1998 Increased expression of the sodium/iodide symporter in papillary thyroid carcinomas. J Clin Invest 101:1296–1300
34. **Saito T, Endo T, Kawaguchi A, Ikeda M, Nakazato M, Kogai T, Onaya T** 1997 Increased expression of the Na+/I− symporter in cultured human thyroid cells exposed to thyrotropin and in Graves' thyroid tissue. J Clin Endocrinol Metab 82:3331–3336
35. **Barnett PS, Banga JP, Watkins J, Huang GC, Gluckman DR, Page MJ, McGregor AM** 1990 Nucleotide sequence of the alternatively spliced human thyroid peroxidase cDNA, TPO-2. Nucleic Acids Res 18:670
36. **Nakajima H, Kim YB, Terano H, Yoshida M, Horinouchi S** 1998 FR901228, a potent antitumor antibiotic, is a novel histone deacetylase inhibitor. Exp Cell Res 241:126–133
37. **Yoshida M, Kijima M, Akita M, Beppu T** 1990 Potent and specific inhibition of mammalian histone deacetylase both *in vivo* and *in vitro* by trichostatin A. J Biol Chem 265:17174–17179
38. **Grunstein M** 1997 Histone acetylation in chromatin structure and transcription. Nature 389:349–352
39. **Maxon HR, Thomas SR, Hertzberg VS, Kereiakes JG, Chen IW, Sperling MI, Saenger EL** 1983 Relation between effective radiation dose and outcome of radioiodine therapy for thyroid cancer. N Engl J Med 309:937–941
40. **Fagin JA, Tang SH, Zeki K, Di Lauro R, Fusco A, Gonsky R** 1996 Reexpression of thyroid peroxidase in a derivative of an undifferentiated thyroid carcinoma cell line by introduction of wild-type p53. Cancer Res 56:765–771
41. **Schmutzler C** 2001 Regulation of the sodium/iodide symporter by retinoids—a review. Exp Clin Endocrinol Diabetes 109:41–44
42. **Venkataraman GM, Yatin M, Marcinek R, Ain KB** 1999 Restoration of iodide uptake in dedifferentiated thyroid carcinoma: relationship to human Na+/I− symporter gene methylation status. J Clin Endocrinol Metab 84:2449–2457
43. **Kitazono M, Robey R, Zhan Z, Sarlis NJ, Skarulis MC, Aikou T, Bates S, Fojo T** 2001 Low concentrations of the histone deacetylase inhibitor, depsipeptide (FR901228), increase expression of the Na(+)/I(−) symporter and iodine accumulation in poorly differentiated thyroid carcinoma cells. J Clin Endocrinol Metab 86:3430–3435
44. **Kitazono M, Chuman Y, Aikou T, Fojo T** 2001 Construction of gene therapy vectors targeting thyroid cells: enhancement of activity and specificity with histone deacetylase inhibitors and agents modulating the cyclic adenosine 3′,5′-monophosphate pathway and demonstration of activity in follicular and anaplastic thyroid carcinoma cells. J Clin Endocrinol Metab 86:834–840
45. **Degroot LJ, Niepomniszcze H** 1977 Biosynthesis of thyroid hormone: basic and clinical aspects. Metabolism 26:665–718
46. **Ekholm R, Bjorkman U** 1984 Localization of iodine binding in the thyroid gland *in vitro*. Endocrinology 115:1558–1567
47. **Ekholm R, Bjorkman U** 1997 Glutathione peroxidase degrades intracellular hydrogen peroxide and thereby inhibits intracellular protein iodination in thyroid epithelium. Endocrinology 138:2871–2878
48. **Huang M, Batra RK, Kogai T, Lin YQ, Hershman JM, Lichtenstein A, Sharma S, Zhu LX, Brent GA, Dubinett SM** 2001 Ectopic expression of the thyroperoxidase gene augments radioiodide uptake and retention mediated by the sodium iodide symporter in non-small cell lung cancer. Cancer Gene Ther 8:612–618
49. **Boland A, Magnon C, Filetti S, Bidart JM, Schlumberger M, Yeh P, Perricaudet M** 2002 Transposition of the thyroid iodide uptake and organification system in nonthyroid tumor cells by adenoviral vector-mediated gene transfers. Thyroid 12:19–26
50. **Vettese-Dadey M, Grant PA, Hebbes TR, Crane-Robinson C, Allis CD, Workman JL** 1996 Acetylation of histone H4 plays a primary role in enhancing transcription factor binding to nucleosomal DNA *in vitro*. EMBO J 15:2508–2518
51. **Turner BM** 1993 Decoding the nucleosome. Cell 75:5–8
52. **Kitazono M, Chuman Y, Aikou T, Fojo T** 2002 Adenovirus HSV-TK construct with thyroid-specific promoter: enhancement of activity and specificity with histone deacetylase inhibitors and agents modulating the camp pathway. Int J Cancer 99:453–459
53. **Schmitt TL, Espinoza CR, Loos U** 2001 Transcriptional regulation of the human sodium/iodide symporter gene by Pax8 and TTF-1. Exp Clin Endocrinol Diabetes 109:27–31
54. **Vigushin DM, Coombes RC** 2002 Histone deacetylase inhibitors in cancer treatment. Anticancer Drugs 13:1–13
55. **Rajgolikar G, Chan KK, Wang HC** 1998 Effects of a novel antitumor depsipeptide, FR901228, on human breast cancer cells. Breast Cancer Res Treat 51:29–38
56. **Greenberg VL, Williams JM, Cogswell JP, Mendenhall M, Zimmer SG** 2001 Histone deacetylase inhibitors promote apoptosis and differential cell cycle arrest in anaplastic thyroid cancer cells. Thyroid 11:315–325
57. **Donda A, Javaux F, Van Renterghem P, Gervy-Decoster C, Vassart G, Christophe D** 1993 Human, bovine, canine and rat thyroglobulin promoter sequences display species-specific differences in an *in vitro* study. Mol Cell Endocrinol 90:R23–R26
58. **Senyuk V, Chakraborty S, Mikhail FM, Zhao R, Chi Y, Nucifora G** 2002 The leukemia-associated transcription repressor AML1/MDS1/EVI1 requires CtBP to induce abnormal growth and differentiation of murine hematopoietic cells. Oncogene 21:3232–3240
59. **Sandor V, Bakke S, Robey RW, Kang MH, Blagosklonny MV, Bender J, Brooks R, Piekarz RL, Tucker E, Figg WD, Chan KK, Goldspiel B, Fojo AT, Balcerzak SP, Bates SE** 2002 Phase I trial of the histone deacetylase inhibitor, depsipeptide (FR901228, NSC 630176), in patients with refractory neoplasms. Clin Cancer Res 8:718–728
60. **Schlumberger M, Challeton C, De Vathaire F, Travagli JP, Gardet P, Lumbroso JD, Francese C, Fontaine F, Ricard M, Parmentier C** 1996 Radioactive iodine treatment and external radiotherapy for lung and bone metastases from thyroid carcinoma. J Nucl Med 37:598–605
61. **Schneider AB, Line BR, Goldman JM, Robbins J** 1981 Sequential serum thyroglobulin determinations, 131I scans, and 131I uptakes after triiodothyronine withdrawal in patients with thyroid cancer. J Clin Endocrinol Metab 53:1199–1206
62. **Schlumberger M, Mancusi F, Baudin E, Pacini F** 1997 131I therapy for elevated thyroglobulin levels. Thyroid 7:273–276

***Endocrinology*** **is published monthly by The Endocrine Society (http://www.endo-society.org), the foremost professional society serving the endocrine community.**

JOURNAL OF BONE AND MINERAL RESEARCH
Volume 17, Number 12, 2002


# Familial Hypocalciuric Hypercalcemia Caused by an R648stop Mutation in the Calcium-Sensing Receptor Gene

MIKA YAMAUCHI,[1] TOSHITSUGU SUGIMOTO,[1] TORU YAMAGUCHI,[1] SHOZO YANO,[1] JUNNING WANG,[2] MEI BAI,[2] EDWARD M. BROWN,[2] and KAZUO CHIHARA[1]

## ABSTRACT

**In this study, we report an 84-year-old female proband in a Japanese family with familial hypocalciuric hypercalcemia (FHH) caused by an R648stop mutation in the extracellular calcium-sensing receptor (CaR) gene. At the age of 71 years, she presented with hypercalcemia (11.4 mg/dl), hypocalciuria (Cca/Ccr = 0.003), hypermagnesemia (2.9 mg/dl), and a high-serum parathyroid hormone (PTH) level (midregion PTH, 3225 [160–520] pg/ml). At the age of 74 years, a family screening was carried out and revealed a total of 9 hypercalcemic individuals (all intact PTH values <62 pg/dl) among 17 family members tested, thus, being diagnosed as FHH. Two and one-half of three clearly enlarged parathyroid glands were resected, because persistently high PTH levels (intact PTH, 292 pg/ml; midregion PTH, 5225 pg/ml) and the presence of a markedly enlarged parathyroid gland by several imaging modalities (ultrasonography, computed tomography [CT], magnetic resonance imaging [MRI], and subtraction scintigraphy) suggested coexistent primary hyperparathyroidism (pHPT); however, hypercalcemia persisted postoperatively. Histological and immunohistochemical examination revealed that the resected parathyroid glands showed lipohyperplasia as well as normally expressed Ki67, vitamin D receptor (VDR), and the CaR. Sequence analysis disclosed that the proband and all affected family members had a heterozygous nonsense (R648stop) mutation in the CaR gene. This mutation is located in the first intracellular loop; thus, it would be predicted to produce a truncated CaR having only one transmembrane domain (TMD) and lacking its remaining TMDs, intracellular loops, and C-terminal tail. Western analysis of biotinylated HEK293 cells transiently transfected with this mutant receptor showed cell surface expression of the truncated protein at a level comparable with that of the wild-type CaR. The mutant receptor, however, exhibited no increase in intracellular free calcium concentration ($Ca^{2+}_i$) when exposed to high extracellular calcium concentrations ($Ca^{2+}_o$). The proband's clinical course was complicated because of associated renal tubular acidosis (RTA) and nephrotic syndrome. However, it was unclear whether their association affected the development of elevated serum PTH and parathyroid gland enlargement. This report is the first to show that an R648stop CaR mutation yields a truncated receptor that is expressed on the cell surface but is devoid of biological activity, resulting in FHH. (J Bone Miner Res 2002;17:2174–2182)**

Key words: **familial hypocalciuric hypercalcemia, calcium-sensing receptor, parathyroid gland, parathyroid hormone, renal tubular acidosis**

## INTRODUCTION

THE EXTRACELLULAR CALCIUM-SENSING receptor (CaR) is a plasma membrane, G protein–coupled receptor that belongs to the superfamily of the seven-transmembrane receptors. The receptor is activated by an increase in the extracellular calcium concentration ($Ca^{2+}_o$) and mainly controls parathyroid hormone (PTH) secretion from the parathyroid gland as well as calcium reabsorption by the kidney.[1–3] Familial hypocalciuric hypercalcemia (FHH) and neonatal severe hyperparathyroidism (NSHPT) are caused by inactivating mutations of the CaR gene on chromosome 3q21–24. FHH results mainly from an inactivating mutation in one CaR allele, whereas NSHPT can be the result of either

The authors have no conflict of interest.

[1]Division of Endocrinology/Metabolism, Neurology, and Hematology/Oncology, Department of Clinical Molecular Medicine, Kobe University Graduate School of Medicine, Kobe, Japan.
[2]Endocrine-Hypertension Division and Membrane Biology Program, Department of Medicine, Brigham and Women's Hospital, Harvard Medical School, Boston, Massachusetts, USA.

heterozygous, compound heterozygous, or homozygous mutations. In contrast, activating mutations lead to autosomal dominant hypoparathyroidism (ADH) and some cases of sporadic hypoparathyroidism.[4-7] FHH patients are characterized by relative hypocalciuria as well as inappropriately normal or slightly elevated serum levels of PTH in spite of hypercalcemia.

Accumulating evidence also supports the involvement of the CaR in regulating the proliferation of parathyroid cells. In secondary hyperparathyroidism (sHPT) caused by chronic renal failure, there is not only PTH hypersecretion but also parathyroid hyperplasia. In the parathyroid glands of rats with experimentally induced chronic renal failure, parathyroid cellular proliferation was inhibited by a high concentration of $Ca^{2+}_o$ in one study.[8] CaR knockout mice also had enlarged parathyroid glands.[9] Moreover, in a rat model of renal failure, CaR agonists suppressed the progression of sHPT as well as parathyroid growth.[8] Because CaR expression in parathyroid cells of patients with sHPT is known to be diminished,[2,10,11] these findings suggest that reduced expression of the CaR may lead to parathyroid growth. In contrast, clinical studies showed that parathyroid glands in FHH patients with certain types of mutant CaR were also occasionally enlarged,[12-14] but it remains unclear whether or not inactivated mutant CaRs in this disorder are the cause of the enlarged parathyroid glands.

Here, we report an elderly patient with a heterozygous R648stop mutation in the CaR that produced a truncated CaR lacking most of its transmembrane and intracellular domains and exhibiting no intracellular $Ca^{2+}$ ($Ca^{2+}_i$) responses to high $Ca^{2+}_o$. This is the second case of this mutation in the literature[15] but the first to show that this CaR mutation yields a truncated receptor that is indeed expressed on the cell surface but is devoid of biological activity, resulting in FHH. Moreover, the patient showed three clearly enlarged parathyroid glands with a markedly increased serum PTH level, suggesting the occasional link between inactivation of the cytoplasmic tail of the CaR and enhanced parathyroid growth.

## MATERIALS AND METHODS

### *Subjects*

An elderly Japanese female with FHH and 17 other family members were studied. An additional group of 50 normal Japanese subjects was recruited as controls. This study complied with the Declaration of Helsinki and was ethically approved by the Institutional Review Board of our institution. Subjects agreed to participate in this study and gave their informed consent.

### *Biochemical measurements*

Serum concentrations of Ca, P, and Cr as well as urinary concentrations of Ca and Cr were measured by automated techniques at the central laboratory of Kobe University Hospital. Intact PTH and midregion PTH were measured by immunoradiometric assay (Allegro Intact PTH RIA kit; normal range, 10–65 pg/ml; Nichols Institute Diagnostics, San Juan Capistrano, CA, USA)[16,17] and radioimmunoassay (RIA; Yamasa hypersenseitive PTH-RIA kit; normal range, 160–520 pg/ml; Yamasa Shoyu Co., Ltd., Tokyo, Japan),[18] respectively. The Yamasa PTH-RIA kit consists of chicken PTH antiserum raised by Hruska et al., $^{125}$I-labeled {$Tyr^{43}$} human PTH(44-68) [hPHT(44-68)] as the radioligand, and synthetic hPTH(1-84) as the standard.[19] The assay recognizes fragments containing the amino acid sequence of at least 44-68 in the PTH molecule as well as intact PTH.

### *Histological examination*

Parathyroid tissues from patients with primary HPT (pHPT; adenoma) and FHH patients were obtained during parathyroidectomy. Normal parathyroid glands, resected together with thyroid tissue in patients with thyroid carcinoma whose renal function was normal, were employed as normal controls. The anti-human CaR antibody, kindly provided by Dr. K. Rogers (NPS Pharmaceuticals, Salt Lake City, UT, USA), was a mouse monoclonal antibody against residues 214–235 (ADD) of the human CaR extracellular domain, as previously described.[20] A rat monoclonal anti-human vitamin D receptor (VDR) antibody (9A7r.E10.E4) and a rabbit affinity-purified, anti-human Ki67 antigen were purchased from NeoMarkers (Fremont, CA, USA) and DAKO (Glostrup, Denmark), respectively. Immunohistochemical staining was performed using formalin-fixed and paraffin-embedded sections as we have previously described.[21] Sections were deparaffinized in xylene and dehydrated through an ethanol series. Then, endogenous peroxidase was inactivated with 0.3% $H_2O_2$ in methanol for 20 minutes at room temperature. After washing twice with PBS, sections were processed in distilled $H_2O$ for 10 minutes using a medical microwave (MI-77; Higashiya, Tokyo, Japan) at 400 W for VDR and Ki67 staining.[22] After blocking with 1.5% nonfat dry milk in PBS for 10 minutes, sections were incubated with each primary antibody overnight at 4°C: ADD (diluted 1:1200 in PBS containing 1% nonimmunized mouse serum), 9A7r (diluted 1:50), or anti-Ki67 antigen (diluted 1:100). After washing thoroughly with PBS, samples were incubated with a biotinylated link antibody (containing anti-rabbit and anti-mouse immunoglobulins) followed by peroxidase-labeled streptavidin using the LSAB2 kit (Dako Corp., Carpinteria, CA, USA) for 30 minutes, respectively. Final development was carried out with 3,3-diaminobenzidine (DAB) containing 0.1% $H_2O_2$ in PBS for 10 minutes.[23] Slides were counterstained with hematoxylin for 30 s only for CaR staining. For staining of VDR and Ki67-antigen, $Ni^{2+}$ and $Co^{2+}$ were added to the DAB solution at 0.3% final concentrations, respectively. Negative controls were carried out using preimmune mouse serum. The intensity of the staining with each of the three antisera was standardized with positive and negative controls. Good reproducibility of the staining intensity was obtained in serial sections. Finally, we quantified the intensity of these signals by visual examination.

### *DNA extraction*

Genomic DNA was extracted from peripheral blood lymphocytes using the GENOMIX kit (TALENT, Triaste, Italy).

*Polymerase chain reaction amplification*

The CaR gene was amplified by polymerase chain reaction (PCR). Exons 2, 3, 5, and 6 were amplified using one specific primer set and exons 4 and 7 were amplified with several primer sets.[24,25] The following primer pairs were used, with the forward primer given first and the reverse primer given second: 5′-TCCCTTGCCCTGGAGAGACGGCAGA-3′ and 5′-AGAGAAGAGATTGGCAGATTAGGCC-3′ for exon 2; AGCTTCCCATTTTCTTCCACTTCTT and CCCGTCTGAGAAGGCTTGAGTACCT for exon 3; ACTCATTCACCATGTTCTTGGTTCT and CCACATGCTGGATCTCTTCC, CCGAGAGGAAGCTGAGGAAAG and CCCAACTCTGCTTTATTATATCAGCA, and CCCAGGAAGTCTGTCCACAATG and CCCAACTCTGCTTTATTATATCAGCA for exon 4; GGCTTGTACTCATTCTTTGCTCCTC and GACATCTGGTTTTCTGATGGACAGC for exon 5; CAAGGACCTCTGGACCTCCCTTTGC and GACCAAGCCCTGCACAGTGCCCAAG for exon 6; and AGTCTGTGCCACACAATAAC and CAGCAGGAACTGCAGGTTGAG. TTCCGCAACACACCCATTGTCAAGG and GAAGAAGCAGATGGCAGC, ACCGCGCCCCCCTCAAGCTA and GGATCCCGTGGAGCCTCCAAGGCTG, and TGCCGTAGAGGTGATTGCCATCCTG and TCTTCCTCAGAGGAAAGGAGTCTGG for exon 7. PCRs were performed with slight modifications of previously reported methods[5] in a final volume of 20 $\mu$l containing 10 pmol each of PCR primer, 2 $\mu$l of 10× buffer (100 mM of Tris-HCl, pH 8.3, 500 mM of KCl, and 15 mM of $MgCl_2$, Takara PCR amplification kit; Takara Shuzo Co., Seta, Japan), 200 $\mu$M of each deoxynucleoside triphosphate (dNTP), 0.5 U of *Taq* polymerase, and 0.5 $\mu$g of genomic DNA in a DNA thermocycler Gene E (Techne, Cambridge, UK) for 35 cycles. DNA was denatured at 94°C for 5 minutes in the first cycle and for 30 s in all subsequent cycles. Annealing was performed at 60°C for 30 s, and elongation was performed at 72°C for 2 minutes, with a final elongation of 10 minutes in the last cycle.

*Sequence analysis of the CaR gene*

The PCR products were sequenced directly using fluorescently labeled primers on an ABI automated DNA sequencing machine (Perkin-Elmer Applied Biosystems, Japan, Tokyo, Japan) according to the manufacturer's instructions.

*Restriction enzyme digestion*

To confirm that the single base change at codon 648 found by direct sequencing analysis was present in only one allele of the CaR gene, the PCR products from exon 7 of the family members and the 50 normal controls were digested with restriction enzyme *Dde*I (New England BioLabs, Beverly, MA), and the predicted molecular sizes of the resultant fragments were assessed by electrophoresis through a 2% agarose gel.

*Transient expression of the wild-type CaR and mutated receptor*

To produce this mutation, site-directed mutagenesis was performed using the approach described previously.[26] The full-length wild-type and mutant receptors were cloned into the mammalian expression vector pcDNA3 (Invitrogen Corp., Carlsbad, CA, USA). The human embryonic kidney cell line (HEK293 cells) was transiently transfected with a wild-type or mutant receptor using pcDNA3 as a vector.[26]

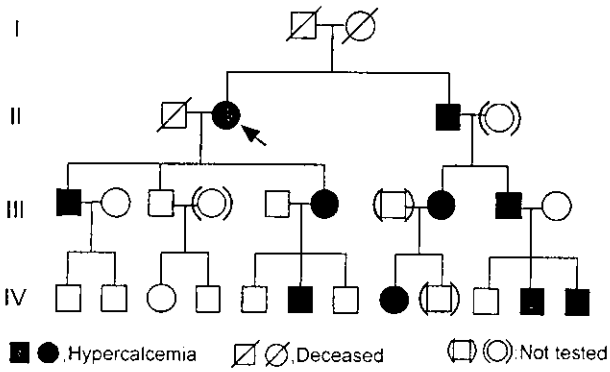


FIG. 1. The pedigree of the Japanese family with FHH.

TABLE 1. LABORATORY DATA OF CALCIUM METABOLISM IN ALL AFFECTED FAMILY MEMBERS

| *Member* | *Age (year)* | *Serum Ca (mg/dl; nl. 8.4–9.9)* | *Serum P (mg/dl; nl. 2.4–4.5)* | *Cca/Ccr* |
|---|---|---|---|---|
| II-1 | 74 | 11.4 | 3.0 | 0.003 |
| II-2 | 71 | 11.1 | 2.5 | 0.009 |
| III-1 | 50 | 10.5 | 2.3 | 0.005 |
| III-3 | 43 | 10.0 | 3.0 | 0.008 |
| III-4 | 44 | 10.9 | 1.6 | 0.008 |
| III-5 | 42 | 11.1 | 2.9 | 0.001 |
| IV-6 | 14 | 10.6 | 4.1 | 0.002 |
| IV-8 | 21 | 11.6 | 2.9 | 0.003 |
| IV-11 | 12 | 11.3 | 4.2 | 0.004 |
| IV-12 | 7 | 11.2 | 3.8 | 0.002 |

*Western analysis of the human CaR expressed on the cell surface*

As described previously,[27] the CaR-transfected cells were surface-biotinylated and the FLAG-tagged CaR in whole cell lysates was immunopurified with anti-FLAG antibody. Then, the immunopurified sample was subjected to SDS-containing PAGE[12] using a linear gradient of polyacrylamide (3–10%). The proteins on the gel were subsequently electrotransferred to a nitrocellulose membrane. After blocking with 5% milk, the forms of the receptor present on the cell surface were detected using an avidin-horseradish peroxidase conjugate (Bio-Rad, Hercules, CA, USA) followed by visualization of the biotinylated bands with an enhanced chemiluminescence (ECL) system (Amersham, Arlington Heights, IL, USA).[26]

*Measurement of $Ca^{2+}{}_i$ by fluorometry*

HEK293 cells that had been transfected with wild-type or mutant CaR cDNA were loaded with fura-2. $CaCl_2$ was added to give the desired final concentrations. The 340/380

TABLE 2. LABORATORY DATA OF PROBAND

| | | | | | |
|---|---|---|---|---|---|
| Blood count | | | | | |
| WBC | 4000/mm$^3$ (4000–8500) | | | | |
| RBC | 299 × 10$^4$/mm$^3$ (380–480) | Hb | 8.9 g/dl (11.8–15.0) | Hct | 29.0% (35.0–44.5) |
| MCV | 93 fl (85–98) | MCH | 29.9 pg (27.0–32.0) | MCHC | 32.1% (32.0–36.0) |
| Plt | 26.1 × 10$^4$/mm$^3$ (13.0–30.0) | | | | |
| Chemist | | | | | |
| t-Bil | 0.3 mg/dl (0.3–1.0) | GOT | 14 IU/liter (9–36) | GTP | 7 IU/liter (7–34) |
| ALP | 215 IU/liter (100–303) | LDH | 314 IU/liter (117–205) | LAP | 35 IU/liter (35–76) |
| γ-GTP | 8 IU/liter (9–64) | TP | 6.9 g/dl (6.5–7.8) | Alb | 3.5 g/dl (4.1–5.0) |
| BUN | 24 mg/dl (9–22) | Cr | 1.2 mg/dl (0.5–1.3) | UA | 6.7 mg/dl (2.6–5.1) |
| Na | 140 mEq/liter (137–146) | K | 5.7 mEq/liter (3.5–4.7) | Cl | 116 mEq/liter (99–109) |
| FPG | 78 mg/dl (61–92) | CPK | 20 IU/liter (35–169) | | |
| Ca | 11.4 mg/dl (8.4–9.9) | P | 3.0 mg/dl (2.4–4.5) | Mg | 2.9 mg/dl (1.7–2.3) |
| intact-PTH | 292 pg/ml (10–65) | midregion PTH | 5225 pg/ml (160–520) | | |
| u-Ca | 8.05 mg/day (100–300) | CCa/CCr | 0.003 | Ccr | 50 ml/minute |
| %TRP | 83% (85–95) | $TmPO_4$/GFR | 2.49 mg/dl (2.55–3.53) | | |
| $1.25(OH)_2D_3$ | 26 pg/ml (20–60) | $25(OH)D_3$ | 22.9 ng/ml (9–33.9) | | |
| N-cAMP | 3.74 nmol/dl (<3.2) | | | | |
| Arterial blood gas analysis | | | | | |
| pH | 7.323 (7.38–7.46) | $PCO_2$ | 33.3 mm Hg (32–46) | $PO_2$ | 83.9 mm Hg (74–108) |
| $HCO_3$ | 16.9 mmol/liter (21–29) | B.E. | −7.9 mmol/liter (−2 − +2) | | |
| Endocrinological examinations | | | | | |
| PRA | 0.6 ng/ml per h (0.3–2.9) | PAC | 162.9 pg/ml (47–131) | | |

Ranges within parentheses are the normal ones.

FPG, fasting plasma glucose; %TRP, tubular reabsorption of phosphate; $TmPO_4$/GFR, tubular maximum reabsorption of phosphate/glomerular filtration rate; N-cAMP, nephrogenous cAMP; B.E., base excess; PRA, plasma renin activity; PAC, plasma aldosterone concentration.

excitation ratio of emitted light was used to calculate $Ca^{2+}{}_i$ as described previously.[26] $EC_{50}$ was defined as the effective concentration of $Ca^{2+}{}_o$ giving one-half of the maximal response. The mean $EC_{50}$ for the wild-type receptor in response to increasing concentrations of $Ca^{2+}{}_o$ was calculated from the $EC_{50}$ values for all the individual experiments and expressed with the SE of the mean.

*Case report*

A 74-year-old female proband in a Japanese family was admitted to our hospital for evaluation of hypercalcemia. Since 1964, she had been followed for nephrotic syndrome and hypertension. At the age of 71 years, she presented with hypercalcemia (11.4 mg/dl), hypermagnesemia (2.9 mg/dl), elevated serum PTH levels (midregion PTH, 3225 pg/ml; normal range, 160–520 pg/ml), and hypocalciuria (Cca/Ccr = 0.003) despite her hypercalcemia. At the age of 74 years, family screening revealed a total of 9 hypercalcemic and hypocalciuric persons among 17 family members tested (Fig. 1; Table 1). One family member (III-3) showed a serum calcium level of 10 mg/dl, which was only slightly higher than the normal range at our institution (8.4–9.9 mg/dl). However, her calcium level was 10.6 mg/dl on another occasion. In contrast, serum calcium levels of 8 unaffected family members were 8.5–9.3 mg/dl. Moreover, we also diagnosed affected family members by the combination of hypercalcemia and hypocalciuria (i.e., low Cca/Ccr; Table 1). Thus, a diagnosis of FHH was established. Her serum PTH levels steadily increased (midregion PTH, 5225 pg/ml; intact PTH, 292 pg/ml) and enlargement of the right lower parathyroid gland was found by several parathyroid imaging techniques (ultrasonography, computed tomography [CT], magnetic resonance imaging [MRI], and subtraction scintigraphy). On admission, her height and weight were 151 cm and 53 kg, respectively. Blood pressure was 160/84 mm Hg. Physical examination was otherwise unremarkable.

Laboratory data on the proband are shown in Table 2 and revealed hyperkalemia, metabolic acidosis, and elevated serum aldosterone levels; type IV renal tubular acidosis (RTA) was diagnosed by a sodium bicarbonate loading test (data not shown).[28] The bone mineral density (BMD) of the lumbar spine measured using a Hologic QDR-1000 densitometer (Hologic, Inc., Waltham, MA, USA) indicated severe osteoporosis (0.638 g/cm$^2$; T score, −3.58; Z score, −0.54). She underwent parathyroid exploration because of the concern that coexistent pHPT was the cause of her

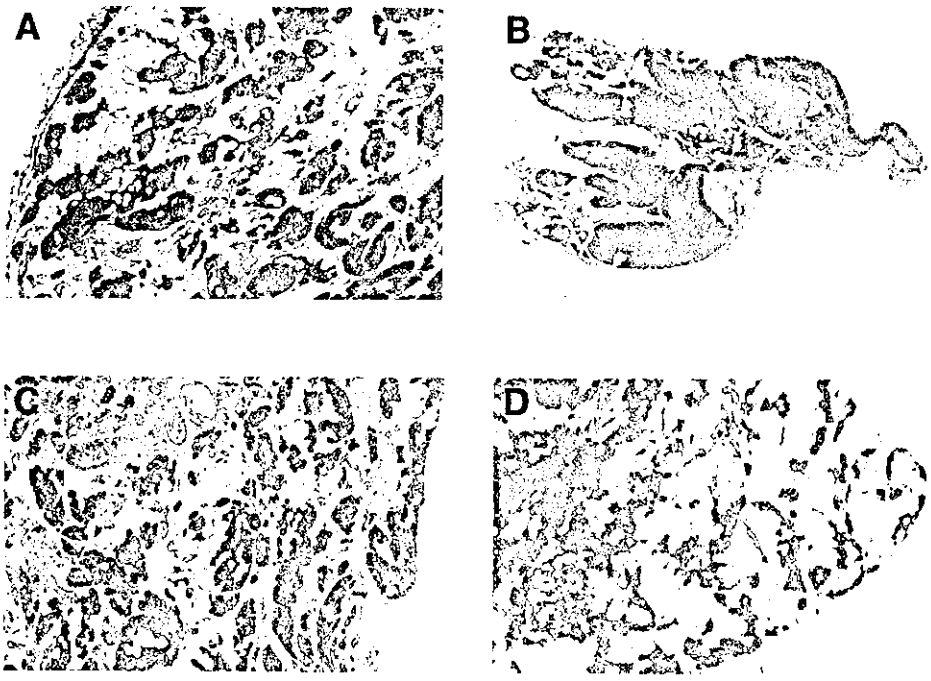


FIG. 2. Composite indicating the correct positions of fragments of the proband's parathyroid tissue removed at the time of parathyroidectomy (top left, right upper; bottom left, right lower; top right, left upper; bottom right, left lower). The three clearly enlarged parathyroid glands showed characteristics of lipohyperplasia, an admixture of fat, and parathyroid chief cells in a 1–2:1 ratio. The normal-sized left upper gland exhibited hyperplasia. (hematoxylin and eosin stain; original magnification ×20).

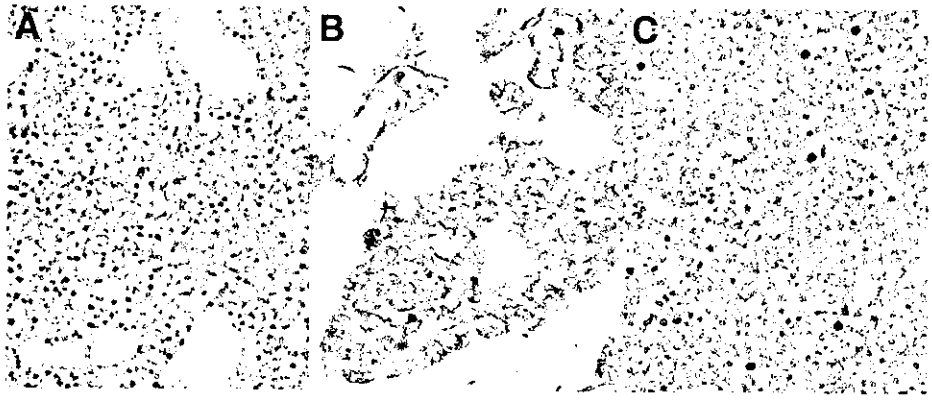


FIG. 3. Immunohistochemistry for Ki67 (from left to right: normal, this case, and pHPT). The parathyroid gland in a patient with pHPT showed many positive cells for Ki67. In contrast, there were no positive cells in a normal parathyroid gland and only one positive cell was shown in the parathyroid gland in the present patient.

persistently high PTH levels and the presence of parathyroid enlargement by imaging. Three of her parathyroid glands, with the sole exception of the left upper gland, were clearly enlarged, and the two glands on the right (both 280 mg in weight) and one-half of the left lower gland were resected. The normal-sized left upper gland was biopsied. Despite the parathyroid resection, hypercalcemia persisted. Therefore, we further examined the histology of the resected parathyroid glands and the gene structure of the patient's CaR.

## RESULTS

### *Histological examination*

Histology of the resected parathyroid glands (right upper, right lower, and left lower) showed the characteristics of lipohyperplasia; namely, there was an admixture of fat and parathyroid chief cells in a 1–2:1 ratio (Fig. 2). The normal-sized left upper gland exhibited hyperplasia (Fig. 2). The gland with lipohyperplasia was assessed further by immunohistochemistry. The parathyroid gland in a patient with pHPT showed many cells that were positive for Ki67, and there were no positive cells in normal parathyroid tissue (Fig. 3). The expressions of VDR and CaR immunoreactivity in normal parathyroid gland were high in the nucleus and the cell surface, respectively, compared with negative controls. The levels of VDR and CaR expressions were markedly decreased in the parathyroid glands in pHPT, compared with normal parathyroid tissue (Figs. 4 and 5). These results were compatible with previous reports.[29–31] In this FHH patient, there were normal levels of expressions of Ki67 (Fig. 3), VDR (Fig. 4), and the CaR (Fig. 5).

### *Mutation in CaR gene*

Nucleotide sequencing of PCR products from the proband disclosed a heterozygous CGA to TGA mutation at codon 648 in exon 7 that resulted in the conversion of the wild-type codon for arginine to a stop codon. The R648stop

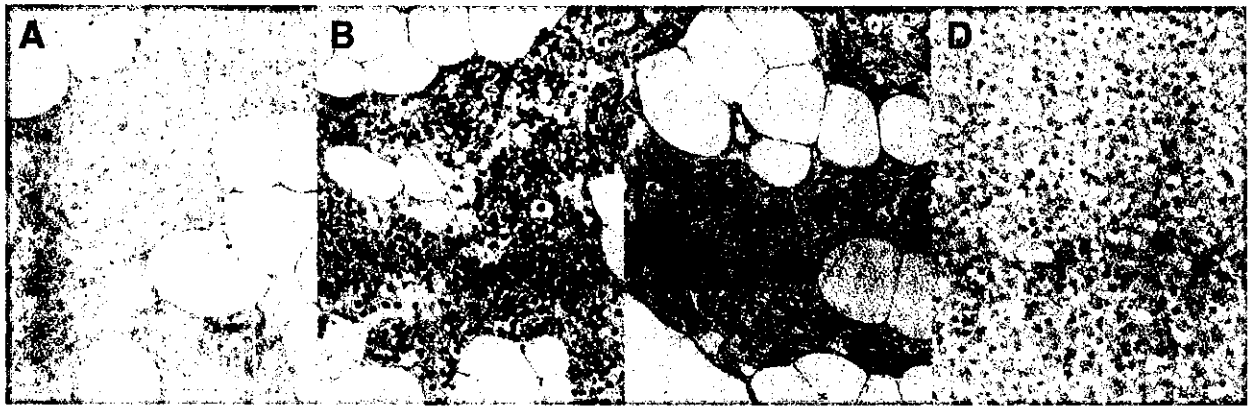


FIG. 4. Immunohistochemistry for VDR (from left to right: negative control, normal, this case, and pHPT). VDR immunoreactive expression of normal parathyroid grand was high in the nucleus, compared with the negative control. The expression of the VDR was markedly decreased in the parathyroid gland from the patient with pHPT, compared with a normal parathyroid gland. The parathyroid gland from the present patient exhibited a normal VDR expression level.

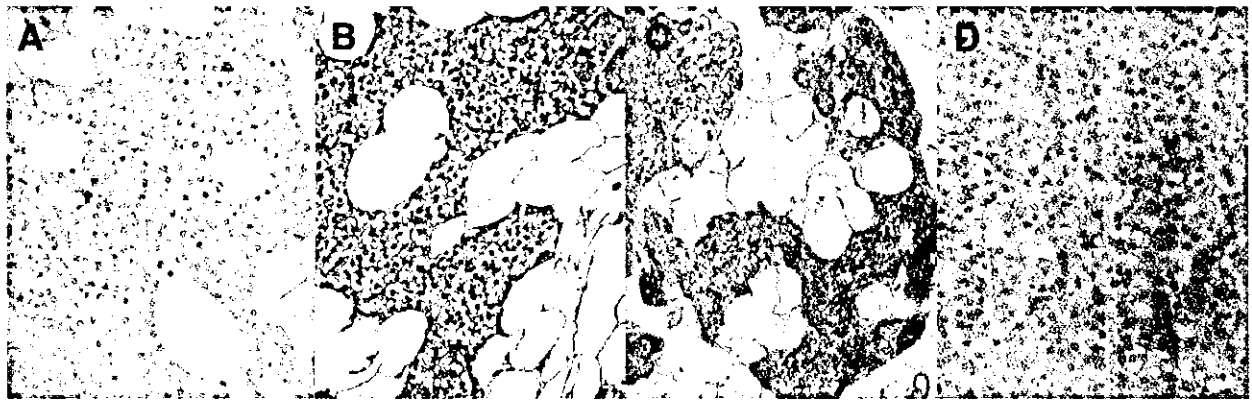


FIG. 5. Immunohistochemistry for the CaR (from left to right: negative control, normal, this case, and pHPT). CaR immunoreactive expression of normal parathyroid grand was high on the cell surface, compared with the negative control. The expression of the CaR was markedly decreased in the parathyroid gland from the patient with pHPT, compared with a normal parathyroid gland. The parathyroid gland from the present patient exhibited a normal CaR expression level.

nonsense mutation had a restriction cleavage site for the *Dde*I restriction enzyme. The proband and affected family members showed both a wild-type PCR product and an additional digested band, confirming that they harbored this heterozygous nonsense mutation. The PCR products of unaffected family members, in contrast, were not cleaved (data not shown). Restriction analysis of PCR products from 50 normal subjects all showed a wild-type pattern (data not shown). These results strongly suggested that the R648stop transition is not a benign polymorphism, but the cause of the derangements in calcium metabolism in this family. This mutation is located in the first intracellular loop and would be predicted to produce a truncated CaR having only one transmembrane domain (TMD) and lacking its remaining TMDs, intracellular loops, and C-terminal tail.

### *Western analysis of the CaR expressed in HEK293 cells*

Western analysis of membrane from biotinylated HEK293 cells transiently transfected with this mutant receptor revealed cell surface expression of the truncated protein at a level comparable with that of the wild-type CaR (Fig. 6).

### *Functional characterization of the R648stop CaR mutation*

The $EC^{50}$ of the wild-type CaR was 3.1 mM as previously reported.[26,32] The mutant receptor exhibited no $Ca^{2+}{}_i$ responses when exposed to high $Ca^{2+}{}_o$ (Fig. 7).

## DISCUSSION

Normal adult parathyroid histology often exhibits an admixture of mature fat cells with parathyroid parenchymal cells in a 1:1 ratio. In contrast, hyperplastic or adenomatous parathyroid tissue in HPT contains no or diminished numbers of mature signet ring adipocytes. In this case, histological examination of the resected parathyroid glands showed

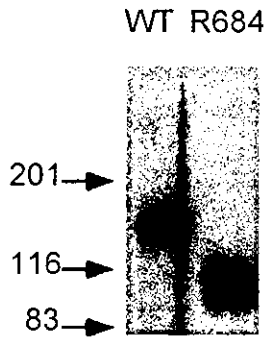


FIG. 6. Western analysis of wild-type and mutant receptors. Western analysis of biotinylated HEK293 cells transiently transfected with this mutant receptor revealed cell surface expression of the truncated protein at a level comparable with that of the wild-type CaR. The left arrows show molecular weight markers in kilodaltons.

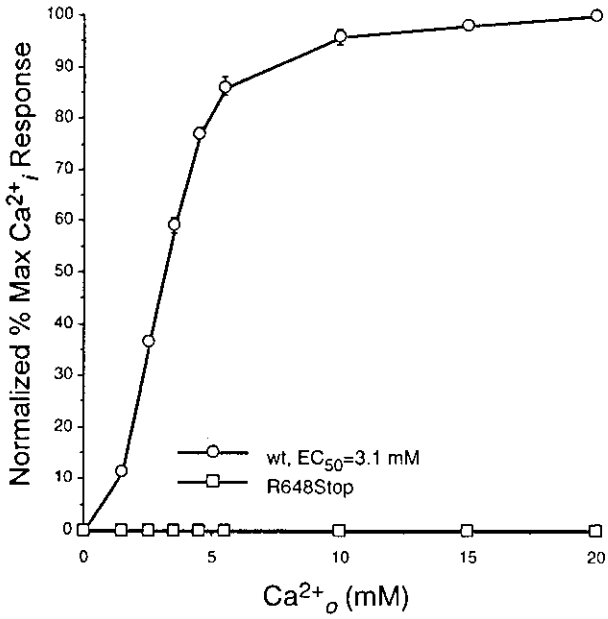


FIG. 7. Functional characterization of the R648stop CaR mutation. Wild-type and mutant CaR cDNAs were transiently transfected into HEK293 cells and increases in $Ca^{2+}_i$ were measured. The $EC_{50}$ of the wild-type receptor was 3.1 mM, which was similar to previous reports. In contrast, the mutant receptor exhibited no $Ca^{2+}_i$ responses when exposed to high $Ca^{2+}_o$.

the characteristics of lipohyperplasia, which is thought to be rather characteristic of the parathyroid glands of patients with FHH.[12,33,34] In contrast, in both pHPT and sHPT, the expression of Ki67, which is a marker for cell proliferation, increases,[35,36] while those of the VDR[21,31,37] and CaR[2,10,12,21] decrease. In this case, the use of immunocytochemistry for detection of Ki67, VDR, and the CaR showed that their expression levels were similar to those of a normal parathyroid gland. Taken together, the histological characteristics of the resected parathyroid glands in this patient were more similar to those of FHH than those of HPT, and thus it is unlikely that persistently high PTH levels and parathyroid enlargement in this patient were explained by coexistence of pHPT.

Homozygous inactivation of the CaR is associated with increased parathyroid cell proliferation (i.e., in CaR knockout mice[9] and patients with NSHPT due to inactivation of both alleles of the CaR), implicating the CaR in regulating parathyroid cellular proliferation. Although inactivation of a single allele of the CaR is not always associated with obvious parathyroid cellular hyperplasia, in some cases heterozygous inactivation of the CaR is associated with parathyroid enlargement.[13,14,38] In these cases it is possible that only certain types of CaR mutations produce enhanced parathyroid growth. Available data indicate that the minimum number of residues in the human CaR required for biological action of the human CaR is somewhere between 877 and 888 and that there are structural elements within regions of the receptor's COOH tail distal to residue 892 that reduce its cell surface expression.[2,4] A mutant CaR with insertion of an Alu-repetitive element at codon 876 resulted in truncated protein that had molecular masses some 30 kDa less than that of the wild-type CaR and exhibited no $Ca^{2+}_i$ responses to either $Ca^{2+}_o$ or $Gd^{3+}_o$. Three of 36 heterozygous gene carriers in an FHH family with this mutation developed high serum calcium and PTH levels, and parathyroid gland enlargement was confirmed at the time of parathyroidectomy.[40,41] In another family exhibiting a heterozygous F881L mutation of the CaR gene, 9 persons among 20 affected family members showed parathyroid hyperplasia or adenoma.[42] These findings suggest that the cytoplasmic tail of the CaR may be important for the suppression of parathyroid cell proliferation and that the loss of its function may induce parathyroid enlargement.

In our case, the R648stop CaR mutation is located in the first intracellular loop and would produce a truncated CaR having only one TMD and lacking its remaining TMDs, intracellular loops, and C-terminal tail. Although the cell surface expression level of the truncated receptor was comparable with that of the wild-type receptor, it was devoid of biological activity with no $Ca^{2+}_i$ responses to high $Ca^{2+}_o$. We examined one of the proband's sons by ultrasonography and found a high-echoic parathyroid mass that implied the presence of a lipohyperplastic gland. Thus, although no affected family member except for the proband showed markedly increased serum PTH levels, all 10 heterozygous gene carriers developed high serum calcium and at least 2 of them exhibited parathyroid enlargement. Thus, our case also supports the notion that abolishing the biological activity of the cytoplasmic tail of the CaR is occasionally, but not consistently, linked to enhanced parathyroid growth. However, we cannot rule out that loss of the intervening intracellular loops and TMDs also participated in this process.

It is unclear whether or not the coexistence of type IV RTA and nephrotic syndrome with FHH in this patient may have contributed to the elevated serum PTH level and the parathyroid gland enlargement. Serum PTH levels are sometimes elevated in RTA because of hypercalciuria and relative hypocalcemia as a result of acidemia,[43] but this is not the case in this patient, because she presented with the opposite biochemical derangements (i.e., hypercalcemia and hypocalciuria). At present, her elevated PTH levels persist despite improvement of her nephrotic syndrome.

Therefore, it is also unlikely that nephrotic syndrome is responsible for her high PTH levels. The same mutation as in the present case has already been reported in a 79-year-old male Chinese patient with hypercalcemia (11.3–11.4 mg/dl) and hypocalciuria (Cca/Ccr = 0.0045–0.0054)[15] who showed a normal range of intact PTH and had no evidence of parathyroid enlargement at neck exploration. He had no family history and no surviving relatives. Therefore, it was unknown whether this mutation was familial or sporadic. Moreover, this previous study lacked functional characterization of the mutant CaR in vitro using receptor-transfected cells, and no parathyroid histology was reported. Thus, our report is the first to show clearly that an R648stop CaR mutation yields a truncated receptor that can be associated with lipohyperplasia and is expressed at normal levels but is devoid of biological activity, resulting in FHH.

## ACKNOWLEDGMENTS

The work is supported in part by grants-in-aid from the Ministry of Science, Education, and Culture of Japan (12671087) as well as the Research Society for Metabolic Bone Disease and from The Hormone Receptor Abnormality Research Committee, Ministry of Health and Welfare of Japan. E.M.B. is supported by NIH grants (DK41415, DK48330, and DK52005) as well as the St. Giles Foundation and NPS Pharmaceuticals.

## REFERENCES

1. Brown EM, Gamba G, Riccardi D, Lombardi M, Butters R, Kifor O, Sun A, Hediger MA, Lytton J, Hebert SC 1993 Cloning and characterization of an extracellular $Ca^{(2+)}$-sensing receptor from bovine parathyroid. Nature **366**:575–580.
2. Chattopadhyay N, Mithal A, Brown EM 1996 The calcium-sensing receptor: A window into the physiology and pathophysiology of mineral ion metabolism. Endocr Rev **17**:289–307.
3. Yamaguchi T, Chattopadhyay N, Brown EM 2000 G protein-coupled extracellular $Ca^{2+}$ ($Ca^{2+}_o$)-sensing receptor (CaR): Roles in cell signaling and control of diverse cellular functions. Adv Pharmacol **47**:209–253.
4. Pollak MR, Brown EM, Chou YH, Hebert SC, Marx SJ, Steinmann B, Levi T, Seidman CE, Seidman JG 1993 Mutations in the human $Ca^{(2+)}$-sensing receptor gene cause familial hypocalciuric hypercalcemia and neonatal severe hyperparathyroidism. Cell **75**:1297–1303.
5. Lovlie R, Eiken HG, Sorheim JI, Boman H 1996 The $Ca^{(2+)}$-sensing receptor gene (PCAR1) mutation T151M in isolated autosomal dominant hypoparathyroidism. Hum Genet **98**: 129–133.
6. Pollak MR, Brown EM, Estep HL, McLaine PN, Kifor O, Park J, Hebert SC, Seidman CE, Seidman JG 1994 Autosomal dominant hypocalcaemia caused by a $Ca^{(2+)}$-sensing receptor gene mutation. Nat Genet **8**:303–307.
7. Pollak MR, Chou YH, Marx SJ, Steinmann B, Cole DE, Brandi ML, Papapoulos SE, Menko FH, Hendy GN, Brown EM, Seidman CE, Seidman JG 1994 Familial hypocalciuric hypercalcemia and neonatal severe hyperparathyroidism. Effects of mutant gene dosage on phenotype. J Clin Invest **93**:1108–1112.
8. Wada M, Furuya Y, Sakiyama J, Kobayashi N, Miyata S, Ishii H, Nagano N 1997 The calcimimetic compound NPS R-568 suppresses parathyroid cell proliferation in rats with renal insufficiency. Control of parathyroid cell growth via a calcium receptor. J Clin Invest **100**:2977–2983.
9. Ho C, Conner DA, Pollak MR, Ladd DJ, Kifor O, Warren HB, Brown EM, Seidman JG, Seidman CE 1995 A mouse model of human familial hypocalciuric hypercalcemia and neonatal severe hyperparathyroidism. Nat Genet **11**:389–394.
10. Brown EM 1997 Mutations in the calcium-sensing receptor and their clinical implications. Horm Res **48**:199–208.
11. Cetani F, Picone A, Cerrai P, Vignali E, Borsari S, Pardi E, Viacava P, Naccarato AG, Miccoli P, Kifor O, Brown EM, Pinchera A, Marcocci C 2000 Parathyroid expression of calcium-sensing receptor protein and in vivo parathyroid hormone-$Ca^{(2+)}$ set-point in patients with primary hyperparathyroidism. J Clin Endocrinol Metab **85**:4789–4794.
12. Law WM Jr, Carney JA, Heath H III 1984 Parathyroid glands in familial benign hypercalcemia (familial hypocalciuric hypercalcemia). Am J Med **76**:1021–1026.
13. Lyons TJ, Crookes PF, Postlethwaite W, Sheridan B, Brown RC, Atkinson AB 1986 Familial hypocalciuric hypercalcaemia as a differential diagnosis of hyperparathyroidism: Studies in a large kindred and a review of surgical experience in the condition. Br J Surg **73**:188–192.
14. Thorgeirsson U, Costa J, Marx SJ 1981 The parathyroid glands in familial hypocalciuric hypercalcemia. Hum Pathol **12**:229–237.
15. Jap TS, Wu YC, Jenq SF, Won GS 2001 A novel mutation in the calcium-sensing receptor gene in a Chinese subject with persistent hypercalcemia and hypocalciuria. J Clin Endocrinol Metab **86**:13–15.
16. Frolich M, Walma ST, Paulson C, Papapoulos SE 1990 Immunoradiometric assay for intact human parathyroid hormone: Characteristics, clinical application and comparison with a radio-immunoassay. Ann Clin Biochem **27**:69–72.
17. Nussbaum SR, Zahradnik RJ, Lavigne JR, Brennan GL, Nozawa-Ung K, Kim LY, Keutmann HT, Wang CA, Potts JT Jr, Segre GV 1987 Highly sensitive two-site immunoradiometric assay of parathyrin, and its clinical utility in evaluating patients with hypercalcemia. Clin Chem **33**:1364–1367.
18. Fukase M, Fujita T, Matsumoto T, Ogata E, Iijima T, Takezawa J, Saito K, Ishige H, Fujimoto M 1989 Clinical studies using a highly sensitive radioimmunoassay for mid-region and carboxy terminus of parathyroid hormone in normal, hypo- and hypercalcemic states (in Japanese). Nippon Naibunpi Gakkai Zasshi **65**:807–827.
19. Hruska KA, Kopelman R, Rutherford WE, Klahr S, Slatopolsky E, Greenwalt A, Bascom T, Markham J 1975 Metabolism in immunoreactive parathyroid hormone in the dog. The role of the kidney and the effects of chronic renal disease. J Clin Invest **56**:39–48.
20. Goldsmith PK, Fan G, Miller JL, Rogers KV, Spiegel AM 1997 Monoclonal antibodies against synthetic peptides corresponding to the extracellular domain of the human $Ca^{2+}$ receptor: Characterization and use in studying concanavalin A inhibition. J Bone Miner Res **12**:1780–1788.
21. Yano S, Sugimoto T, Tsukamoto T, Chihara K, Kobayashi A, Kitazawa S, Maeda S, Kitazawa R 2000 Association of decreased calcium-sensing receptor expression with proliferation of parathyroid cells in secondary hyperparathyroidism. Kidney Int **58**:1980–1986.
22. Lan HY, Mu W, Nikolic-Paterson DJ, Atkins RC 1995 A novel, simple, reliable, and sensitive method for multiple immunoenzyme staining: Use of microwave oven heating to block antibody crossreactivity and retrieve antigens. J Histochem Cytochem **43**:97–102.
23. Hsu SM, Raine L, Fanger H 1981 Use of avidin-biotin-peroxidase complex (ABC) in immunoperoxidase techniques: A comparison between ABC and unlabeled antibody (PAP) procedures. J Histochem Cytochem **29**:577–580.

24. Chikatsu N, Fukumoto S, Suzawa M, Tanaka Y, Takeuchi Y, Takeda S, Tamura Y, Matsumoto T, Fujita T 1999 An adult patient with severe hypercalcaemia and hypocalciuria due to a novel homozygous inactivating mutation of calcium-sensing receptor. Clin Endocrinol (Oxf) **50**:537–543.
25. Pearce SH, Trump D, Wooding C, Besser GM, Chew SL, Grant DB, Heath DA, Hughes IA, Paterson CR, Whyte MP, Thakker RV 1995 Calcium-sensing receptor mutations in familial benign hypercalcemia and neonatal hyperparathyroidism. J Clin Invest **96**:2683–2692.
26. Bai M, Quinn S, Trivedi S, Kifor O, Pearce SH, Pollak MR, Krapcho K, Hebert SC, Brown EM 1996 Expression and characterization of inactivating and activating mutations in the human Ca2+o-sensing receptor. J Biol Chem **271**:19537–19545.
27. Bai M, Trivedi S, Brown EM 1998 Dimerization of the extracellular calcium-sensing receptor (CaR) on the cell surface of CaR-transfected HEK293 cells. J Biol Chem **273**:23605–23610.
28. Nagai T, Totsune K, Saito S, Furuyama T 1985 Sodium bicarbonate loading test and urine-blood carbon dioxide partial pressure for the diagnosis of renal tubular acidosis (in Japanese). Nippon Rinsho **43**:1843–1848.
29. Kifor O, Moore FD Jr, Wang P, Goldstein M, Vassilev P, Kifor I, Hebert SC, Brown EM 1996 Reduced immunostaining for the extracellular $Ca^{2+}$-sensing receptor in primary and uremic secondary hyperparathyroidism. J Clin Endocrinol Metab **81**:1598–1606.
30. Gogusev J, Duchambon P, Hory B, Giovannini M, Goureau Y, Sarfati E, Drueke TB 1997 Depressed expression of calcium receptor in parathyroid gland tissue of patients with hyperparathyroidism. Kidney Int **51**:328–336.
31. Sudhaker Rao D, Han ZH, Phillips ER, Palnitkar S, Parfitt AM 2000 Reduced vitamin D receptor expression in parathyroid adenomas: Implications for pathogenesis. Clin Endocrinol (Oxf) **53**:373–381.
32. Pearce SH, Bai M, Quinn SJ, Kifor O, Brown EM, Thakker RV 1996 Functional characterization of calcium-sensing receptor mutations expressed in human embryonic kidney cells. J Clin Invest **98**:1860–1866.
33. Law WM Jr, Heath H III 1985 Familial benign hypercalcemia (hypocalciuric hypercalcemia). Clinical and pathogenetic studies in 21 families. Ann Intern Med **102**:511–519.
34. Fukumoto S, Chikatsu N, Okazaki R, Takeuchi Y, Tamura Y, Murakami T, Obara T, Fujita T 2001 Inactivating mutations of calcium-sensing receptor results in parathyroid lipohyperplasia. Diagn Mol Pathol **10**:242–247.
35. Loda M, Lipman J, Cukor B, Bur M, Kwan P, DeLellis RA 1994 Nodular foci in parathyroid adenomas and hyperplasias: An immunohistochemical analysis of proliferative activity. Hum Pathol **25**:1050–1056.
36. Tominaga Y, Tsuzuki T, Uchida K, Haba T, Otsuka S, Ichimori T, Yamada K, Numano M, Tanaka Y, Takagi H 1999 Expression of PRAD1/cyclin D1, retinoblastoma gene products, and Ki67 in parathyroid hyperplasia caused by chronic renal failure versus primary adenoma. Kidney Int **55**:1375–1383.
37. Korkor AB 1987 Reduced binding of [3H]1,25-dihydroxyvitamin D3 in the parathyroid glands of patients with renal failure. N Engl J Med **316**:1573–1577.
38. Law WM Jr, James EM, Charboneau JW, Purnell DC, Heath H III 1984 High-resolution parathyroid ultrasonography in familial benign hypercalcemia (familial hypocalciuric hypercalcemia). Mayo Clin Proc **59**:153–155.
39. Ray K, Fan GF, Goldsmith PK, Spiegel AM 1997 The carboxyl terminus of the human calcium receptor. Requirements for cell-surface expression and signal transduction. J Biol Chem **272**:31355–31361.
40. Cole DE, Janicic N, Salisbury SR, Hendy GN 1997 Neonatal severe hyperparathyroidism, secondary hyperparathyroidism, and familial hypocalciuric hypercalcemia: Multiple different phenotypes associated with an inactivating Alu insertion mutation of the calcium-sensing receptor gene. Am J Med Genet **71**:202–210.
41. Janicic N, Pausova Z, Cole DE, Hendy GN 1995 Insertion of an Alu sequence in the $Ca^{(2+)}$-sensing receptor gene in familial hypocalciuric hypercalcemia and neonatal severe hyperparathyroidism. Am J Hum Genet **56**:880–886.
42. Carling T, Szabo E, Bai M, Ridefelt P, Westin G, Gustavsson P, Trivedi S, Hellman P, Brown EM, Dahl N, Rastad J 2000 Familial hypercalcemia and hypercalciuria caused by a novel mutation in the cytoplasmic tail of the calcium receptor. J Clin Endocrinol Metab **85**:2042–2047.
43. Lee DB, Drinkard JP, Gonick HC, Coulson WF, Cracchiolo A 1976 Pathogenesis of renal calculi in distal renal tubular acidosis. Possible role of parathyroid hormone. Clin Orthop 234–242.

Address reprint requests to:
*Toshitsugu Sugimoto, M.D., Ph.D.*
*Division of Endocrinology/Metabolism, Neurology, and Hematology/Oncology*
*Department of Clinical Molecular Medicine*
*Kobe University Graduate School of Medicine*
*7–5–1 Kusunoki-cho, Chuo-ku*
*Kobe 650-0017, Japan*

Received in original form February 4, 2002; in revised form May 3, 2002; accepted May 30, 2002.

0021-972X/05/$15.00/0
*Printed in U.S.A.*

The Journal of Clinical Endocrinology & Metabolism 90(1):296–301

doi: 10.1210/jc.2004-0931

# Interleukin-13 Gene Polymorphisms Confer the Susceptibility of Japanese Populations to Graves' Disease

Yuji Hiromatsu, Tomoka Fukutani, Michiko Ichimura, Tokunori Mukai, Hiroo Kaku, Hitomi Nakayama, Ikuyo Miyake, Shingo Shoji, Yoshiro Koda, and Tomasz Bednarczuk

*Department of Endocrinology and Metabolism (Y.H., T.F., M.I., T.M., H.K., H.N., I.M., S.S.) and Division of Human Genetics, Department of Forensic Medicine (Y.K.), Kurume University School of Medicine, Kurume, Fukuoka 830-0011, Japan; and Department of Endocrinology, Medical Research Center, Polish Academy of Science (T.B.), Warsaw, Poland 02-097*

**Graves' disease (GD) is an autoimmune disorder with genetic predisposition. IL-13 is an important mediator of antiinflammatory immune responses and is expressed in the thyroid and orbit. The aim of the present study was to investigate whether IL-13 gene polymorphisms are associated with the development of GD. IL-13 gene polymorphisms were studied in Japanese GD patients (n = 310) and healthy control subjects without antithyroid autoantibodies or a family history of autoimmune disorders (n = 244). A C/T polymorphism at position −1112 of the promoter region was measured using the direct sequencing method, and an $Arg^{130}Gln$ (G2044A) polymorphism in exon 4 was examined using the PCR-restriction fragment length polymorphism method. There was a significant decrease in −1112T allele frequency in GD patients compared with controls (16% *vs.* 23%; $P = 0.0019$). The frequency of the 2044A allele on exon 4 also appeared lower in GD patients compared with controls. Haplotype analysis showed a significant decrease in the −1112T/2044A haplotype in GD patients. There was no association between IL-13 gene polymorphisms and ophthalmopathy, severity, or serum IgE levels. In conclusion, IL-13 gene polymorphisms are associated with GD susceptibility in Japan. (*J Clin Endocrinol Metab* 90: 296–301, 2005)**

GRAVES' DISEASE (GD) is an autoimmune disorder frequently associated with varying degrees of hyperthyroidism and ophthalmopathy (1). Although the TSH receptor has been proposed as an autoantigen in GD patients, the nature of autoimmune reactions in the thyroid and orbit, and the mechanisms linking GD and Graves' ophthalmopathy (GO) have not been fully elucidated (2, 3). Several lines of research support the involvement of environmental factors, such as smoking, and genetic factors in both GD and GO (4–6). The genetic susceptibility of these diseases is thought to be polygenic. It has been reported that major histocompatibility complex gene (7, 8), cytotoxic T lymphocyte antigen-4 gene (9–11), interferon-γ gene (12, 13), and TNF-α gene (14) polymorphisms are associated with GD and GO; however, none of these associations has been fully confirmed.

There is now considerable evidence suggesting that IgE is associated with the severity of Graves' hyperthyroidism (15–17) and GO (18–20). Recent studies of a Japanese population showed that serum IgE concentrations increased by 30–40% in GD patients, correlating with the recurrence of hyperthyroidism after antithyroid drug treatment. IgE deposits and mast cells have also been reported in the thyroid and eye muscle tissues of patients with GD and GO, suggesting that IgE might play a role in autoimmune inflammation (18, 21, 22).

IL-13 is an important immunoregulatory protein produced primarily by activated T helper 2 cells (23) and is involved in B cell maturation. It up-regulates CD23 and major histocompatibility complex class II expression (24) and promotes IgE isotype switching in human B cells (25). IL-13 also down-regulates macrophage activity, thereby inhibiting the production of proinflammatory cytokines and chemokines such as IL-1α, IL-1β, IL-6, IL-8, and TNF-α. Numerous single nucleotide polymorphisms (SNP) have recently been identified in the IL-13 gene and have been found to be associated with IgE levels and/or allergic diseases (26). Thus, IL-13 might be a potential candidate gene contributing to the development of GD or influencing its clinical course. Currently two SNPs in the IL-13 locus have been identified as having a biological function. One is located in the 5′-flanking region at position −1112 (C to T change, termed C-1112T) and has been shown to regulate gene transcription (27, 28). The second is located in exon 4 at position 2044 (G to A change, termed as G2044A) and causes an amino acid exchange (arginine to glutamine at codon 130, termed $Arg^{130}Gln$), which possibly affects ligand/receptor interactions (29, 30). The aim of the present study was to investigate whether IL-13 gene polymorphisms are associated with the development of GD and GO.

## Subjects and Methods

### *Subjects*

In total, 310 GD patients (71 males and 239 females; aged 11–83 yr; mean age, 42.4 ± 15.5 yr) being treated at Kurume University Hospital

First Published Online October 13, 2004

Abbreviations: GD, Graves' disease; GO, Graves' ophthalmopathy; *Pc*, corrected *P*; SNP, single nucleotide polymorphism; TRAb, TSH binding-inhibiting Ig; TSAb, thyroid-stimulating antibody.

were enrolled in this study. GD diagnosis was determined by the presence of hyperthyroidism and serum anti-TSH receptor antibodies [TSH binding-inhibiting immunoglobulin (TRAb) and thyroid-stimulating antibody (TSAb)] and/or an increased $^{123}I$ uptake ratio with diffuse uptake. Ophthalmopathy was classified according to the system recommended by the American Thyroid Association (ATA) committee (31). Ninety-eight of the GD patients (24 males and 74 females) showed ophthalmopathy defined as ATA class III or greater and were classified as GO. Two hundred and twelve patients showed no ophthalmopathy (ATA class 0), signs of ophthalmopathy without symptoms (ATA class I), or only soft tissue involvement (ATA class II). Two hundred and forty-four healthy unrelated Japanese medical students and staffs (97 males and 147 females; aged 18–79 yr; mean age, 30.7 ± 10.6 yr) with no family history of autoimmune diseases and no detectable antithyroid autoantibodies were enrolled as control subjects. The study plan was reviewed and approved by the institutional review committee, and informed consent was obtained from all patients and control subjects.

### *IL-13 gene polymorphism*

Genomic DNA extracted from peripheral blood was subjected to PCR to amplify the polymorphic regions. The promoter region of the IL-13 gene (32) (GenBank accession no. U31120) was amplified by PCR using IL-13 primers originally reported by Laundy *et al.* (33). PCR was performed using 50 ng genomic DNA, 1.25 U *Taq* DNA polymerase (AmpliTaq, Applied Biosystems, Foster City, CA), 0.5 μM of each primer (forward, 5′-TCTGAGCGGGAATCCAGCAT-3′; reverse, 5′-AATGAGTGCTGTGGAG GGCG-3′), 1.5 mM $MgCl_2$, and 200 μM of each deoxynucleotide triphosphate under the following conditions: 35 cycles of PCR consisting of 30 sec at 95 C, annealing for 30 sec at 60 C, extension for 1 min at 72 C, and a final extension for 5 min at 72 C in a thermocycler (PerkinElmer, Gene Amp PCR system 9600, Applied Biosystems). The PCR products were directly sequenced using an ABI sequencer (ABI PRISM 3100 Genetic Analyzer, PerkinElmer, Applied Biosystems) to determine the C/T polymorphism at position −1112 relative to the transcription start site (29).

A 236-bp PCR fragment including the $Arg^{130}Gln$ polymorphism was generated using the following primers: 5′-CTTCCGTGAGGACTGAATGAGACGGTC-3′ and 5′-GCAAATAATGATGCTTTCGAAGTTTCAGTGGA-3′, as previously reported (34). The *underlined* bases were modified to create *Nla*IV restriction sites. PCRs were carried out in a total volume of 50 μl containing approximately 50 ng genomic DNA, 10 mmol/liter Tris-hydrochloric acid (pH 8.3), 2.0 mM $MgCl_2$, 200 μM of each deoxynucleotide triphosphate, 0.5 μM of each primer, and 1.25 U *Taq* DNA polymerase (Applied Biosystems). Samples were denatured at 95 C for 5 min, followed by 33 cycles of 95 C for 30 sec, 60 C for 30 sec, and 72 C for 1 min, and then a final extension for 10 min at 72 C. The PCR products were digested by the addition of 0.25 U *Nla*IV (New England Biolabs, Boston, MA) and incubation at 37 C for 8 h. *Nla*IV digests the PCR fragment 26 bp from the 5′ end, which serves as a control for assessing whether digestion is complete. It also digests 32 bp from the 3′ end of the fragment when the G nucleotide ($Arg^{130}$) is present, producing a 178-bp fragment. The digested PCR products were electrophoresed on 3% agarose gels to separate the fragments.

### *Laboratory test*

Serum concentrations of free $T_3$, free $T_4$, and TSH were determined by enzyme immunoassays. TRAb was measured by radioreceptor assay with a commercial kit (DiaSorin, Inc., Stillwater, MN), and antithyroglobulin and antithyroid peroxidase antibodies were measured by RIA using commercial kits (RSR Ltd., Cardiff, UK). The cut-off values for TRAb, antithyroglobulin antibodies, and antithyroid peroxidase antibodies were 10%, 0.3 kU/liter, and 0.3 kU/liter, respectively. Serum IgE was measured by nephelometric assay (Dade Bering Marburg GmbH, Marburg, Germany).

### *Statistical analysis*

The clinical data were expressed as the mean ± SD. Differences in clinical data between groups were evaluated using a *t* test or Welch's *t* test. Haplotype frequencies were estimated by maximum likelihood using Arlequin software available from the ARLEQUIN website (http://lgb.unige.ch/arlequin/) (35). The statistical significance of any differences in frequency between each polymorphic allele and genotype of the patient and control groups was evaluated using the $\chi^2$ test or Fisher's exact probability test. *P* values were corrected by multiplying by the number of different alleles or haplotypes tested. In this study a corrected *P* (*Pc*) < 0.05 was considered statistically significant.

## Results

### *Association between IL-13 gene polymorphisms and GD*

The distributions of alleles and haplotypes for both groups (control and GD) are in good agreement with the Hardy-Weinberg equilibrium. We calculated pairwise linkage disequilibrium between the promoter and exon 4 variants. These two variants were in significant linkage disequilibrium (by Fisher's exact test, $P < 0.000001$; $D' = 0.803$ in the control and 0.807 in the GD group).

The CC genotype frequencies at position −1112 in the promoter region of the IL-13 gene were significantly greater in GD patients compared with controls (71% *vs.* 59%, respectively; CC genotype *vs.* CT and TT genotypes, $\chi^2 = 8.738$, $P = 0.0031$, $Pc = 0.0186$; Table 1). The C allele frequency at position −1112 in the promoter region of the IL-13 gene was significantly greater in GD patients compared with controls (84% *vs.* 77%; $\chi^2 = 9.611$; $P = 0.0019$; $Pc = 0.0076$; estimated power = 0.85; Table 1). The G allele frequency at position 2044 in exon 4 of the IL-13 gene appeared greater in GD patients than controls, but this difference was not statistically significant (73% *vs.* 67%; $\chi^2 = 5.690$; $P = 0.0171$; $Pc = 0.0684$).

The association of the C-1112T polymorphism of the IL-13 gene with GD was observed when the female GD patients (n = 239) and control subjects (n = 147) were analyzed (C allele frequency; 85% *vs.* 77%; $\chi^2 = 6.512$; $P = 0.0107$; $Pc = 0.0428$; data not shown).

The association was also observed when the nonsmoking GD patients (n = 191) and control subjects (n = 171) were

**TABLE 1.** IL-13 gene polymorphisms in patients with GD and healthy control subjects

| IL-13 gene polymorphism | GD (n = 310) | Control subjects (n = 244) | $\chi^2$ test, *P* value |
|---|---|---|---|
| C-1112T | | | |
| Genotype frequencies | | | |
| CC | 219 (71) | 143 (59) | $\chi^2 = 9.565$ |
| CT | 83 (27) | 88 (36) | $P = 0.0084^a$ |
| TT | 8 (2) | 13 (5) | |
| Allele frequencies | | | |
| C | 521 (84) | 374 (77) | $\chi^2 = 9.611$ |
| T | 99 (16) | 114 (23) | $P = 0.0019^b$ |
| G2044A | | | |
| Genotype frequencies | | | |
| GG | 166 (53) | 113 (46) | $\chi^2 = 6.594$ |
| GA | 123 (40) | 100 (41) | $P = 0.0370^c$ |
| AA | 21 (7) | 31 (13) | |
| Allele frequencies | | | |
| G | 455 (73) | 326 (67) | $\chi^2 = 5.690$ |
| A | 165 (27) | 162 (33) | $P = 0.0171^d$ |

Values in *parentheses* are percentages of the group. *P* values were calculated with $\chi^2$ test, comparing patients with GD and healthy control subjects.

[a] $Pc = 0.0504$.

[b] $Pc = 0.0076$.

[c] $Pc = 0.2220$.

[d] $Pc = 0.0684$.

analyzed (C allele frequency; 85% *vs.* 77%; $\chi^2$ =11.845; $P$ = 0.0027; $Pc$ = 0.0108; data not shown).

Although the distribution of haplotype combinations did not differ between the GD patients and healthy controls ($\chi^2$ = 14.887; $P$ = 0.0614), the −1112C/2044G haplotype frequency was greater in GD patients than in healthy controls ($\chi^2$ = 6.856; $P$ = 0.0088; $Pc$ = 0.0352; Table 2), and the −1112T/2,044A haplotype frequency was significantly less in GD patients than in controls ($\chi^2$ = 8.530; $P$ = 0.0035; $Pc$ = 0.0140; Table 2).

*Association between IL-13 gene polymorphisms and ophthalmopathy*

There was no significant difference in genotype or allele frequencies of IL-13 gene polymorphisms between the patients with evident ophthalmopathy (ATA class III or more; GO) and those without or with mild ophthalmopathy (ATA class 0–II; Table 3). However, the C allele frequency at position −1112 in the promoter region of the IL-13 gene in GO patients was significantly greater than that in controls (87% *vs.* 77%; $\chi^2$ = 8.755; $P$ = 0.0031; $Pc$ = 0.0124; Tables 1 and 3). The G allele frequency at position 2044 in exon 4 of the IL-13 gene was greater in GO patients than in controls (76% *vs.* 67%; $\chi^2$ = 4.983; $P$ = 0.0256; $Pc$ = 0.1024; Tables 1 and 3).

**TABLE 3.** IL-13 gene polymorphisms in patients with GO and in patients with Graves' hyperthyroidism without clinically evident ophthalmopathy

| IL-13 gene polymorphism | Ophthalmopathy | | $\chi^2$ test, $P$ value |
|---|---|---|---|
| | ATA class III–VI (n = 98) | ATA class 0–II (n = 212) | |
| C-1112T | | | |
| Genotype frequencies | | | |
| CC | 74 (76) | 145 (68) | $\chi^2$ = 1.643 |
| CT | 22 (22) | 61 (29) | $P$ = 0.4397 |
| TT | 2 (2) | 6 (3) | |
| Allele frequencies | | | |
| C | 170 (87) | 351 (83) | $\chi^2$ = 1.560 |
| T | 26 (13) | 73 (17) | $P$ = 0.2117 |
| G2044A | | | |
| Genotype frequencies | | | |
| GG | 54 (55) | 112 (53) | $\chi^2$ = 1.645 |
| GA | 40 (41) | 83 (39) | $P$ = 0.4393 |
| AA | 4 (4) | 17 (8) | |
| Allele frequencies | | | |
| G | 148 (76) | 307 (72) | $\chi^2$ = 0.661 |
| A | 48 (24) | 117 (28) | $P$ = 0.4160 |

ATA class, Classification by the American Thyroid Association. Values in *parentheses* are percentages of the group. $P$ values were calculated with $\chi^2$ test, comparing patients with GD with ophthalmopathy and without evident ophthalmopathy.

**TABLE 2.** Haplotype frequency of IL-13 gene polymorphisms in patients with GD and healthy control subjects

| IL-13 gene polymorphism | GD | Control subjects | $\chi^2$ test, $P$ value |
|---|---|---|---|
| Haplotype frequencies (promoter C/T-exon G/A) | n = 620 | n = 488 | |
| CG | 441 (71) | 311 (64) | $\chi^2$ = 10.011 |
| CA | 80 (13) | 63 (13) | $P$ = 0.0185[a] |
| TG | 14 (2) | 15 (3) | |
| TA | 85 (14) | 99 (20) | |
| $CG^{+/-}$ | 441/179 (71) | 311/177 (64) | $\chi^2$ = 6.856 |
| | | | $P$ = 0.0088[b] |
| $CA^{+/-}$ | 80/540 (13) | 63/425 (13) | $\chi^2$ = 0.0001 |
| | | | $P$ = 0.9974 |
| $TG^{+/-}$ | 14/606 (2) | 15/473 (3) | $\chi^2$ = 0.3985 |
| | | | $P$ = 0.713 |
| $TA^{+/-}$ | 85/535 (14) | 99/389 (20) | $\chi^2$ = 8.530 |
| | | | $P$ = 0.0035[c] |
| Haplotype combination | n = 310 | n = 244 | |
| CG/CG | 156 | 101 | $\chi^2$ = 14.887 |
| CG/CA | 60 | 35 | $P$ = 0.0614 |
| CA/CA | 3 | 7 | |
| CG/TG | 10 | 12 | |
| CA/TG | 2 | 2 | |
| CG/TA | 59 | 62 | |
| CA/TA | 12 | 12 | |
| TG/TG | 0 | 0 | |
| TA/TG | 2 | 1 | |
| TA/TA | 6 | 12 | |
| CG/CG or CG/− | 285 | 210 | $\chi^2$ = 4.944 |
| Others | 25 | 34 | $P$ = 0.0262[d] |
| TA/TA or TA/− | 79 | 87 | $\chi^2$ = 6.732 |
| Others | 231 | 157 | $P$ = 0.0095[e] |

Percentages are given in *parentheses*. + or − indicates the presence or absence of particular haplotype.
[a] $Pc$ = 0.0740.
[b] $Pc$ = 0.0352.
[c] $Pc$ = 0.0140.
[d] $Pc$ = 0.1048.
[e] $Pc$ = 0.0380.

**TABLE 4.** Association of IL-13 gene polymorphisms with laboratory features of patients with GD

| IL-13 gene polymorphism | No. | $FT_3$ | | $FT_4$[b] | | TRAb (%) | TSAb (%) |
|---|---|---|---|---|---|---|---|
| | | pg/ml[a] | pmol/liter | ng/dl | pmol/liter | | |
| C-1112T genotype | | | | | | | |
| CC | 127 | 12.9 ± 6.1 | 19.8 ± 6.1 | 4.8 ± 2.6 | 61.8 ± 33.5 | 35.0 ± 24.2[c] | 423 ± 450 |
| CT | 52 | 14.9 ± 8.1 | 22.9 ± 8.1 | 5.9 ± 3.6 | 75.9 ± 33.5 | 39.0 ± 27.6[d] | 609 ± 965 |
| TT | 5 | 13.3 ± 5.4 | 20.4 ± 5.4 | 4.7 ± 1.8 | 60.5 ± 23.2 | 20.6 ± 10.6 | 331 ± 273 |
| G2044A genotype | | | | | | | |
| GG | 94 | 13.4 ± 6.3 | 20.6 ± 6.3 | 5.2 ± 3.1 | 66.9 ± 39.9 | 36.3 ± 255 | 410 ± 449 |
| GA | 78 | 13.4 ± 7.5 | 20.6 ± 7.5 | 5.3 ± 3.2 | 68.2 ± 41.2 | 35.8 ± 25.1 | 492 ± 497 |
| AA | 12 | 13.3 ± 5.9 | 20.4 ± 5.8 | 4.9 ± 2.5 | 63.1 ± 32.2 | 30.8 ± 26.8 | 890 ± 1785 |

No., Number of patients; $FT_3$, free $T_3$; $FT_4$, free $T_4$; TRAb, TSH binding-inhibiting Ig. Values in *parentheses* are expressed as Systeme International (SI) units.

[a] Conversion factor for SI units, multiply conventional units by 1.536 to equal picomoles per liter.

[b] Conversion factor for SI units, multiply conventional units by 12.87 to equal picomoles per liter.

[c] $P = 0.0324$ (by Welch's $t$ test, compared with TT group); $Pc = 0.1944$.

[d] $P = 0.0115$ (by Welch's $t$ test, compared with TT group); $Pc = 0.0690$.

*Association between IL-13 gene polymorphisms and severity of Graves' hyperthyroidism*

There were no significant differences in the levels of serum free $T_4$, free $T_3$, and TSH receptor antibodies among the genotypes of the C-1112T polymorphism or the G2044A polymorphism. However, differences in TRAb levels were observed at the time of diagnosis (Table 4). TRAb titers tended to be low in patients with the TT genotype.

*Association between IL-13 gene polymorphisms and serum IgE levels in GD patients and normal controls*

Serum IgE levels were elevated in 34% of the GD patients at the time of diagnosis or during treatment with antithyroid drugs and in 28% of the control subjects (Table 5). Mean serum IgE levels tended to be greater in the CC and CT genotypes than in the TT genotype at position −1112 of the IL-13 promoter region in GD patients (Table 5). However, this difference was not significant. There was no significant association between the G2044A polymorphisms and serum IgE levels in either GD or control subjects.

When GD patients and control subjects, whose serum IgE levels were less than 170 kIU/liter, were analyzed, the CC genotype and the C allele frequencies at position −1112 of the promoter region of the IL-13 gene were significantly greater in GD patients compared with controls (CC genotype *vs.* CT and TT genotypes: $\chi^2 = 9.405$; $P = 0.0022$; $Pc = 0.0132$; C allele *vs.* T allele frequencies: $\chi^2 = 8.392$; $P = 0.0038$; $Pc = 0.0152$; Table 6).

## Discussion

GD is an organ-specific autoimmune disorder characterized by diffuse goiter and thyroid hormone oversecretion as a result of TSH receptor antibody stimulation. Although the etiology of GD remains unclear, it is believed to be caused by a complex interaction between genetic and environmental factors. Recent genome-wide research has provided evidence for the linkage of GD to loci on multiple chromosomes, including loci on chromosomes 5 in regions 5q31-q33 (36–38), which have been linked to autoimmune thyroid disorders, including GD in Japanese and Chinese populations, but not in Caucasian populations. This might suggest that these loci are specific to eastern Asian populations. The loci in regions 5q31-q33 have also been identified as being susceptible to IgE synthesis (39–42). This region encodes a cluster of cytokine genes, including IL-3, IL-4, IL-5, IL-9, and IL-13, that are involved in inflammation and IgE synthesis (43). Furthermore, IL-13 mRNA expression has been demonstrated in thyroid and orbital tissues from GD patients (44, 45), suggesting that IL-13 might be a potential candidate gene contributing to the development of GD or influencing its clinical severity and course.

Our previous study with a power of 60–85% suggested

**TABLE 5.** Association of IL-13 gene polymorphisms with serum total IgE in patients with GD and control subjects

| IL-13 gene polymorphism | GD | | | Control subjects | | |
|---|---|---|---|---|---|---|
| | IgE >170 kIU/liter (n = 299) | Mean ± SD (kIU/liter) | Median (kIU/liter) | IgE >170 kIU/liter (n = 123) | Mean ± SD (kIU/liter) | Median (kIU/liter) |
| C-1112T genotype | | | | | | |
| CC | 73/213 (34) | 308.5 ± 621.4 | 105 | 22/69 (32) | 276.2 ± 648.7 | 78.2 |
| CT | 29/78 (37) | 327.7 ± 534.8 | 107 | 9/46 (20) | 214.1 ± 463.8 | 76.7 |
| TT | 1/8 (13) | 130.2 ± 235.7[a] | 52.9 | 3/8 (38) | 225.7 ± 227.9 | 101.2 |
| G2044A genotype | | | | | | |
| GG | 55/160 (34) | 281.5 ± 538.0 | 112 | 17/56 (30) | 292.1 ± 710.5 | 81.5 |
| GA | 42/118 (36) | 339.3 ± 651.0 | 84.8 | 13/51 (25) | 222.7 ± 448.9 | 76.0 |
| AA | 6/21 (29) | 345.0 ± 658.2 | 116 | 4/16 (25) | 186.9 ± 221.7 | 75.2 |
| Total | 103/299 (34) | 308.6 ± 592.3 | 103 | 34/123 (28) | 249.7 ± 563.8 | 78.2 |

Values in *parentheses* are percentages of the group.

[a] By Welch's $t$ test, $P = 0.0732$ *vs.* CT group; $P = 0.0832$ *vs.* CC group.

**TABLE 6.** IL-13 gene polymorphisms in patients with GD and healthy control subjects whose serum IgE levels were less than 170 kIU/liter

| IL-13 gene polymorphism | GD (n = 196) | Control subjects (n = 89) | $\chi^2$ test, $P$ value |
|---|---|---|---|
| C-1112T | | | |
| Genotype frequencies | | | |
| CC | 140 (71) | 47 (53) | $\chi^2 = 9.414$ |
| CT | 49 (25) | 37 (41) | $P = 0.0090^a$ |
| TT | 7 (4) | 5 (6) | |
| Allele frequencies | | | |
| C | 329 (84) | 131 (74) | $\chi^2 = 8.392$ |
| T | 63 (16) | 47 (26) | $P = 0.0038^b$ |
| G2044A | | | |
| Genotype frequencies | | | |
| GG | 105 (53) | 39 (44) | $\chi^2 = 3.583$ |
| GA | 76 (39) | 38 (43) | $P = 0.1667$ |
| AA | 15 (8) | 12 (13) | |
| Allele frequencies | | | |
| G | 286 (73) | 116 (65) | $\chi^2 = 3.574$ |
| A | 106 (27) | 62 (35) | $P = 0.0587^c$ |

Values in *parentheses* are percentages of the group. $P$ values were calculated by $\chi^2$ test, comparing patients with GD and healthy control subjects.

[a] $Pc = 0.0540$.

[b] $Pc = 0.0152$.

[c] $Pc = 0.2348$.

that in the Polish-Caucasian population studied, IL-13 gene SNPs at positions −1112 (C→T) and 2044 (G→A), 1) do not confer genetic susceptibility to GD, 2) do not contribute to the development of clinically evident GO, and 3) are not associated with the severity of Graves' hyperthyroidism (34). In the present study a positive association between IL-13 gene polymorphisms and GD was demonstrated for the first time. In this study the C allele frequency in GD patients was significantly greater than that in control subjects. This contradictory result might reflect the insufficient power of the studies or the different genetic susceptibilities of different ethic groups to GD, supporting the idea that the 5q31 locus is specific to eastern Asian populations. Additional large-scale studies are needed to make a definitive conclusion.

IL-13 is an important immunoregulatory protein that plays a role in the regulation of IgE synthesis (43). An IL-13 promoter C to T polymorphism alters the regulation of IL-13 production (27) and possibly contributes to asthma (27, 28). Another polymorphism, the Gln form of $Arg^{130}Gln$, was shown to be associated with increased serum IgE levels in three Caucasian populations (29). In the present study, however, an association between C-1112T or $Arg^{130}Gln$ polymorphisms and serum IgE levels could not be found in either GD patients or control subjects. This discrepancy between studies of Caucasian and Japanese populations with regard to IgE synthesis suggests that different genetic factors influence IgE synthesis in different ethnic groups. The present study also showed that the C allele frequency was significantly greater in GD patients than control subjects even when those with high titers of IgE were excluded from the study. The results, therefore, suggest that IL-13 polymorphisms independently confer susceptibility to GD.

The relationships between IL-13 polymorphisms and the severity of hyperthyroidism and ophthalmopathy were also investigated. There were no differences in IL-13 polymorphism allele frequency between patients with clinically evident ophthalmopathy and patients without ophthalmopathy or those with mild ophthalmopathy. IL-13 gene polymorphisms were likely to be associated with serum levels of TRAb. However, there were no differences in the other clinical markers investigated, namely, free $T_4$, free $T_3$, or TSH receptor antibodies. Additional studies are necessary to determine whether IL-13 polymorphisms are associated with the outcome of antithyroid drug treatments. In conclusion, this study has shown for the first time that IL-13 gene polymorphisms are associated with the development of GD, but not with ophthalmopathy, in Japanese populations.

## Acknowledgments

Received May 17, 2004. Accepted October 1, 2004.

Address all correspondence and requests for reprints to: Dr. Yuji Hiromatsu, Department of Endocrinology and Metabolism, Kurume University School of Medicine, 67 Asahimatchi, Kurume, Fukuoka 830-0011, Japan. E-mail: yuji@med.kurume-u.ac.jp.

This work was supported in part by a grant-in-aid for scientific research from the Ministry of Education, Science, Sports, and Culture, Japan.

## References

1. **Weetman AP** 2000 Graves' disease. N Engl J Med 26:1236–1248
2. **Davies TF** 2000 Causes of thyrotoxicosis. Graves' disease. Pathogenesis. In: Braverman LE, Utiger RD, eds. Werner and Ingbar's the thyroid. Philadelphia: Lippincott Williams and Wilkins; 518–531
3. **Bartalena L, Pinchera A, Marcocci C** 2000 Management of Graves' ophthalmopathy: reality and perspectives. Endocr Rev 21:168–199
4. **Wiersinga WM** 2001 Genetic and environmental contributions to pathogenesis. In: Bahn RS, ed. Thyroid eye disease. Boston: Kluwer; 99–118
5. **Tomer Y** 2002 Genetic dissection of familial autoimmune thyroid diseases using whole genome screening. In: Akamizu T, Kasuga M, Davies TF, eds. The genomics of complex thyroid diseases. Tokyo: Springer-Verlag; 3–22
6. **Vaidya B, Kendall-Taylor P, Pearce SH** 2002 The genetics of autoimmune thyroid disease. J Clin Endocrinol Metab 87:5385–5397
7. **Schleusener H, Schernthaner G, Mayr WR, Kotulla P, Bogner U, Finke R, Meinhold H, Koppenhagen K, Wenzel KW** 1983 HLA-DR3 and HLA-DR5 associated thyrotoxicosis: two different types of toxic diffuse goiter. J Clin Endocrinol Metab 56:781–785
8. **Weetman AP, Zhang L, Webb S, Shine B** 1990 Analysis of HLA-DQB and HLA-DPB alleles in GD by oligonucleotide probing of enzymatically amplified DNA. Clin Endocrinol (Oxf) 33:65–71
9. **Vaidya B, Imrie H, Perros P, Dickinson J, McCarthy MI, Kendall-Taylor P, Pearce SH** 1999 Cytotoxic T lymphocyte antigen-4 (CTLA-4) gene polymorphism confers susceptibility to thyroid associated orbitopathy. Lancet 354: 743–744
10. **Kouki T, Sawai Y, Gardine CA, Fisfalen ME, Alegre ML, DeGroot LJ** 2000 CTLA-4 gene polymorphism at position 49 in exon 1 reduces the inhibitory function of CTLA-4 and contributes to the pathogenesis of Graves' disease. J Immunol 165:6606–6611
11. **Bednarczuk T, Hiromatsu Y, Fukutani T, Jazdzewski K, Miskiewicz P, Osikowska M, Nauman J** 2003 Association of cytotoxic T-lymphocyte-associated antigen-4 (CTLA-4) gene polymorphism and non-genetic factors with Graves' ophthalmopathy in European and Japanese populations. Eur J Endocrinol 148:13–18
12. **Siegmund T, Usadel KH, Donner H, Braun J, Walfish PG, Badenhoop K** 1998 Interferon-γ gene microsatellite polymorphisms in patients with Graves' disease. Thyroid 8:1013–1017
13. **Fukutani T, Hiromatsu Y, Kaku H, Miyake I, Mukai T, Imamura Y, Kohno S, Takane N, Ahoji S, Otabe S, Yamada K** 2004 A polymorphism of interferon γ gene associated with changes of anti-TSH receptor antibodies induced by anti-thyroid drug treatment for Graves' disease in Japanese. Thyroid 14:93–97
14. **Kamizono S, Hiromatsu Y, Seki N, Bednarczuk T, Matsumoto H, Kimura A, Itoh K** 2000 A polymorphism of the 5′ flanking region of tumour necrosis factor α gene is associated with thyroid-associated ophthalmopathy in Japanese. Clin Endocrinol (Oxf) 52:759–764
15. **Sato A, Takemura Y, Yamada T, Ohtsuka H, Sakai H, Miyahara Y, Aizawa T, Terao A, Onuma S, Junen K, Kanamori A, Nakamura Y, Tejima E, Ito Y, Kamijo K** 1999 A possible role of immunoglobulin E in patients with hyperthyroid Graves' disease. J Clin Endocrinol Metab 84:3602–3605